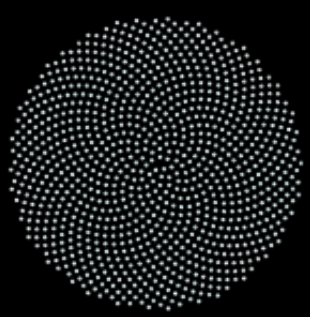

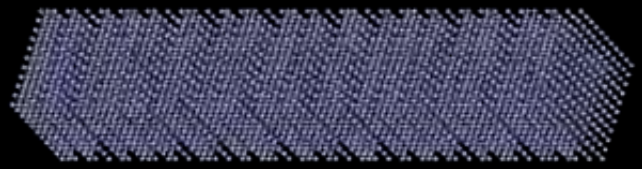
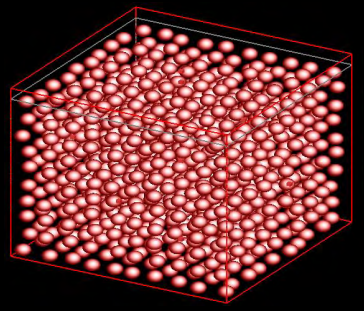

Final Activities Report
Aperiodic Metamaterials

February 26, 2018

Prof. Luca Dal Negro

Department of Electrical and Computer Engineering & Photonics Center, Boston University
8 Saint Mary's Street Boston, Massachusetts 02215, United States

This material is based upon work supported by the Defense Advanced Research Projects Agency under Air Force Contract No. FA8702-15-D-0001. Any opinions, findings, conclusions or recommendations expressed in this material are those of the author(s) and do not necessarily reflect the views of the Defense Advanced Research Projects Agency.

The Boston University photonics center

www.bu.edu/nano

BOSTON UNIVERSITY

Outline

Method developments, validations, and design

- Finite Element Homogenization
  - Papers validation beyond quasi-statics
  - ENZ in dielectrics using Si nanoparticles
- Analytical Mie theory CPA Homogenization
  - Developed CPA homogenization approached for core-shells
  - Core-shell dielectric nanoparticles with doubly negative parameters
  - Nonlinear enhancement with engineered ENZ media
  - Potential fabrication route
- Electric and magnetic dipole modeling and homogenization
  - Method and code development;
  - Analysis of aperiodic scattering arrays;
  - Experimental demonstration of magnetic array resonances;
- Arbitrary k-space control
  - Designed k-space beyond hyper-uniform patters
- Introduced “colored metamaterials” with tunable spatial correlations

Numerical Homogenization: validation with Ag particles

Cell size: a=75nm, R=25nm, **10 Ag periodic spheres along the vertical axis**, effective refractive index comparison with k-k method

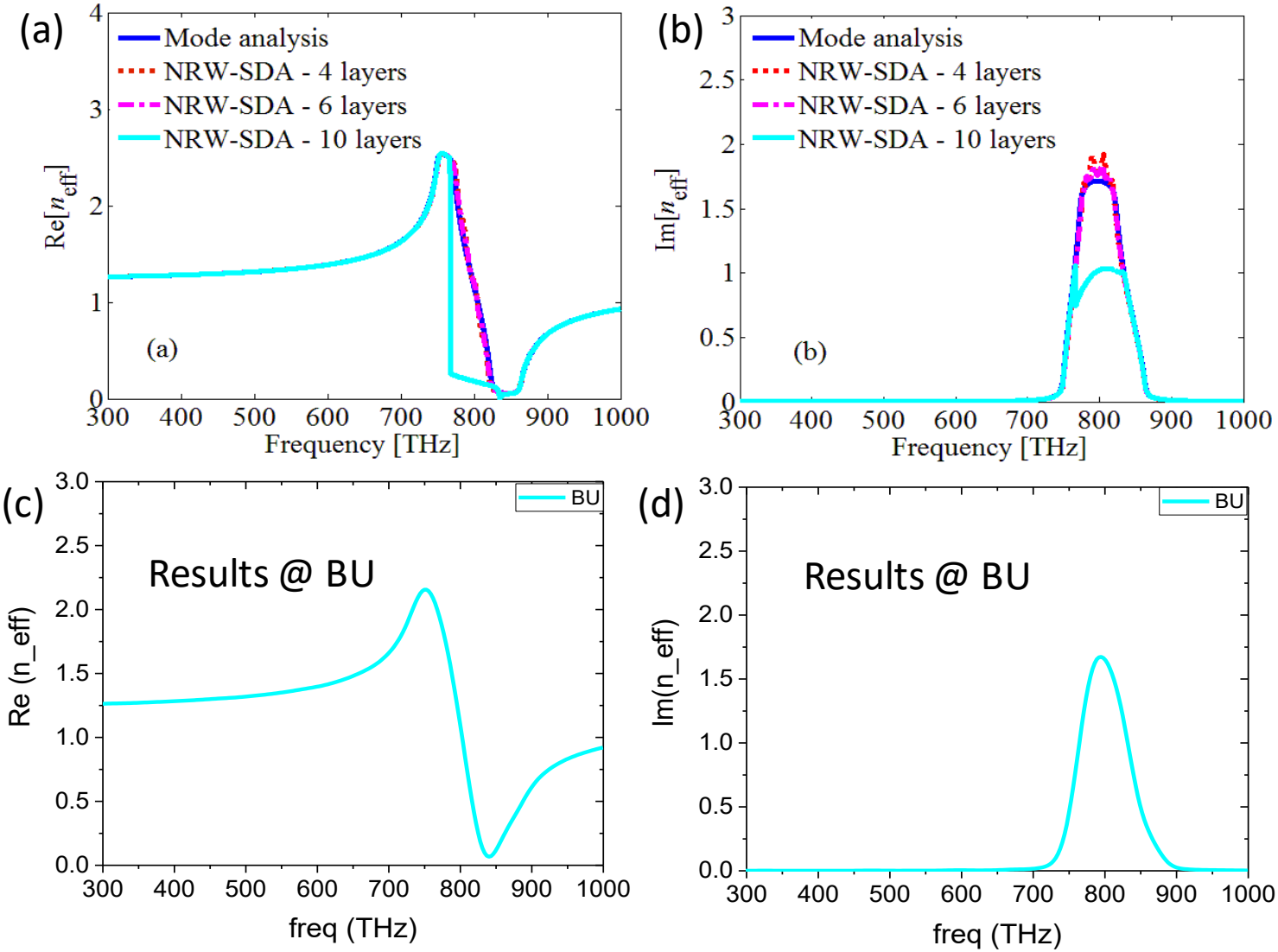

Campione S, Steshenko S, Albani M, et al. Complex modes and effective refractive index in 3D periodic arrays of plasmonic nanospheres. Optics Express, 2011, 19(27):26027-26043.

Developing dielectric ENZ media using Si nanoparticles

Used Si dispersion data cubic unit cell a=400nm radius of spheres R=150nm

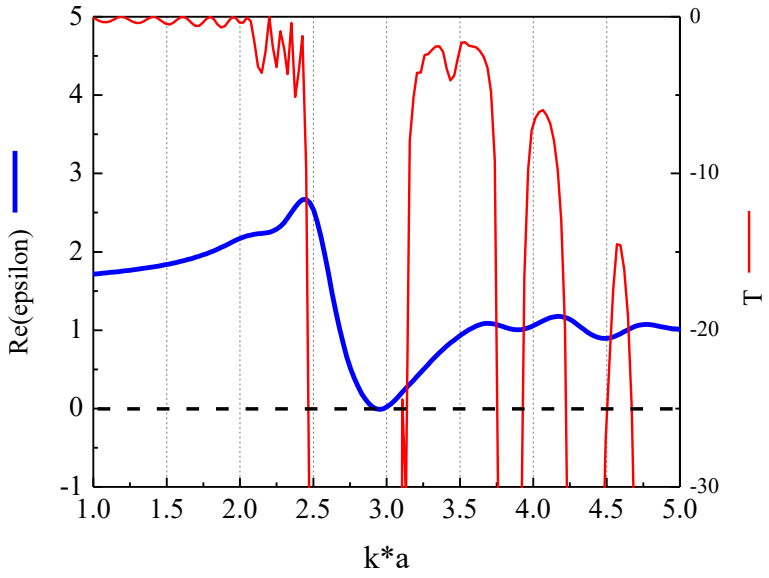

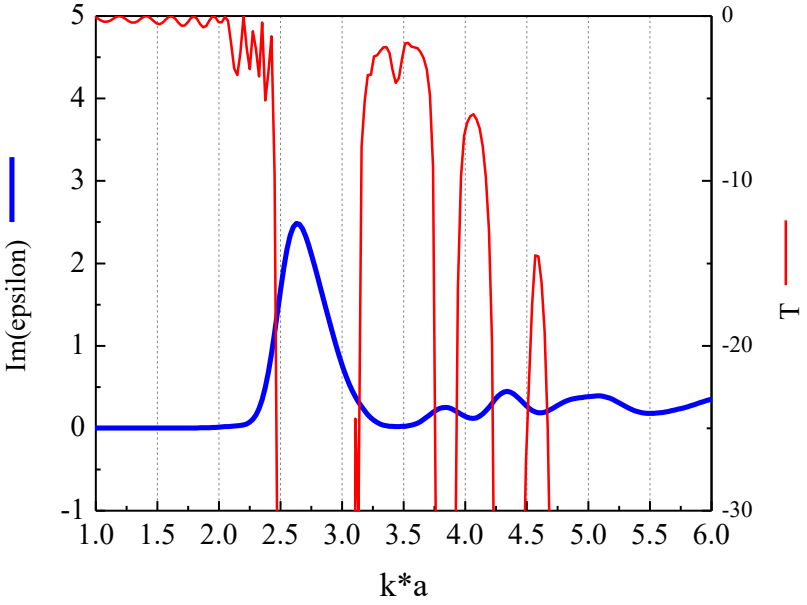

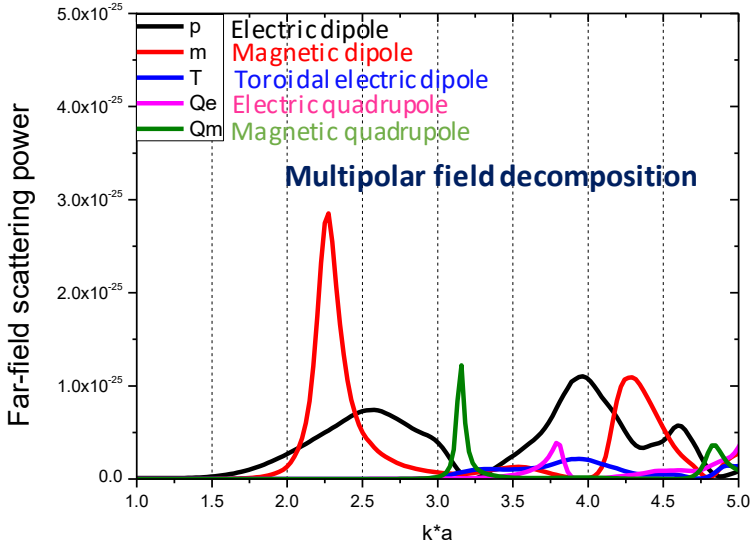

We have engineered a dielectric metamaterial made of Si nanospheres that exhibits effective epsilon close to zero (ENZ) beyond the quasi-static limit (i.e., for size parameter ka=3).

This can open new routes to control light-matter coupling and enhance non-linearity without metals.

Disorder in the unit cell: "Smectic Metamaterials"

Randomization of planes along x-, y-directions in the unit cell: max(δx)=d/3, max(δy)=d/3; Uniform distributions of shifts of the lattice planes

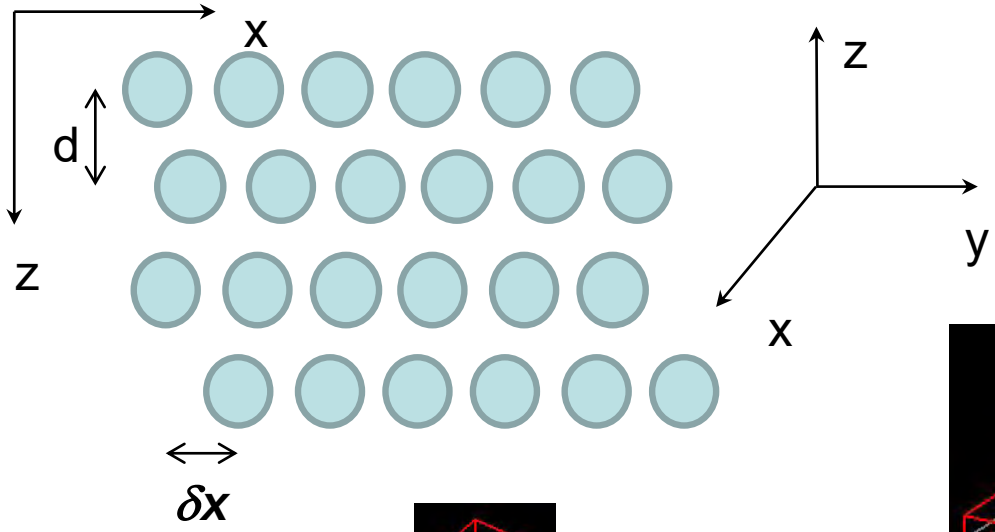

Unit cell

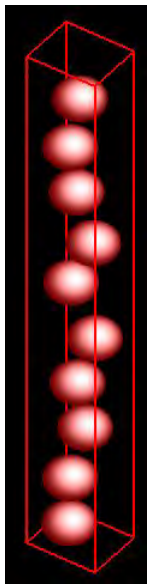

Global structure

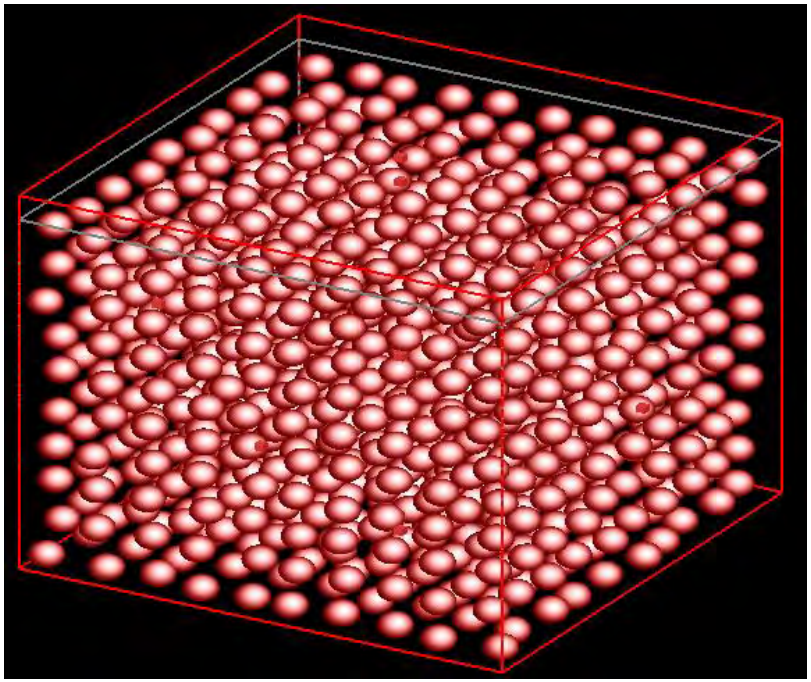

Metallic Spheres: Increasing Randomness

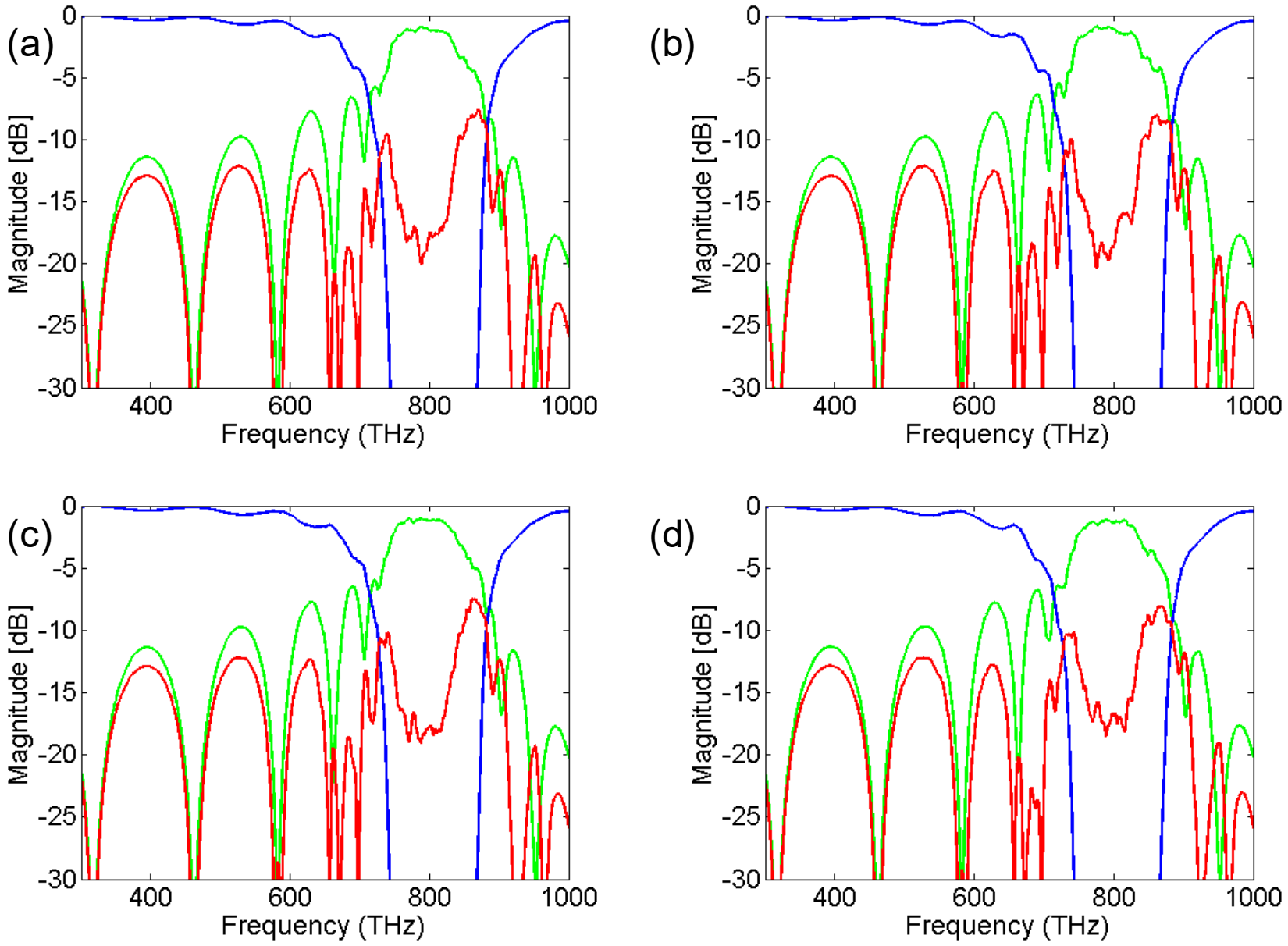

Finite Elements Homogenization of Si spheres, unit cell size a=400nm

(a)

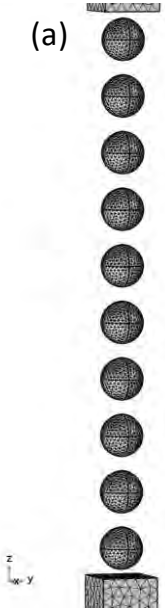

$$Z_{\text{eff}} = \pm\sqrt{\frac{(1+S_{11})^2 - S_{21}^2}{(1-S_{11})^2 - S_{21}^2}}$$

$$e^{iN_{\text{eff}}k_0 d_{\text{eff}}} = \frac{S_{21}}{1 - S_{11}R_{01}}$$

$$n^{\text{KK}}(\omega') = 1 + \frac{2}{\pi}\mathcal{P}\int_0^{\infty}\frac{\omega\kappa_{\text{eff}}(\omega)}{\omega^2 - \omega'^2}\mathrm{d}\omega$$

Szabo Z, et al. IEEE Transactions on Microwave Theory & Techniques, 2010

- Fixed unit cell size a=400nm
- Sweeping Si spheres radius from 40-190nm

(b)

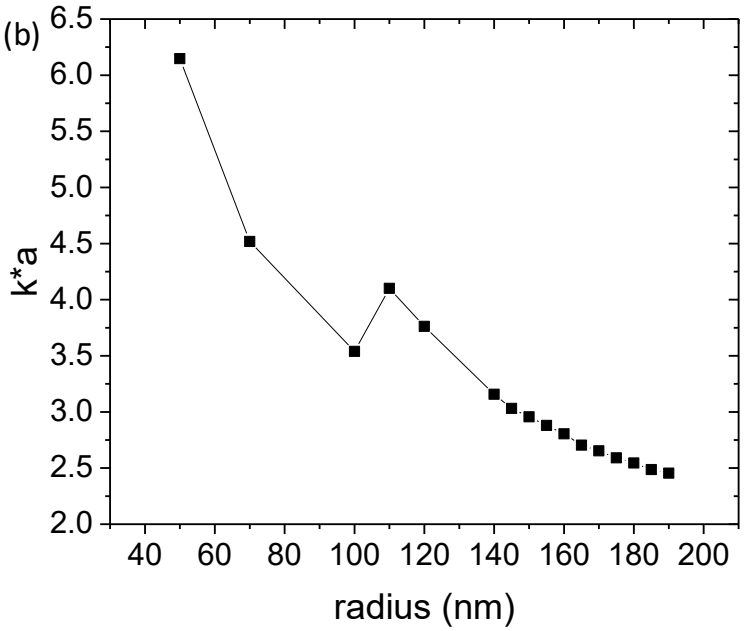

(c)

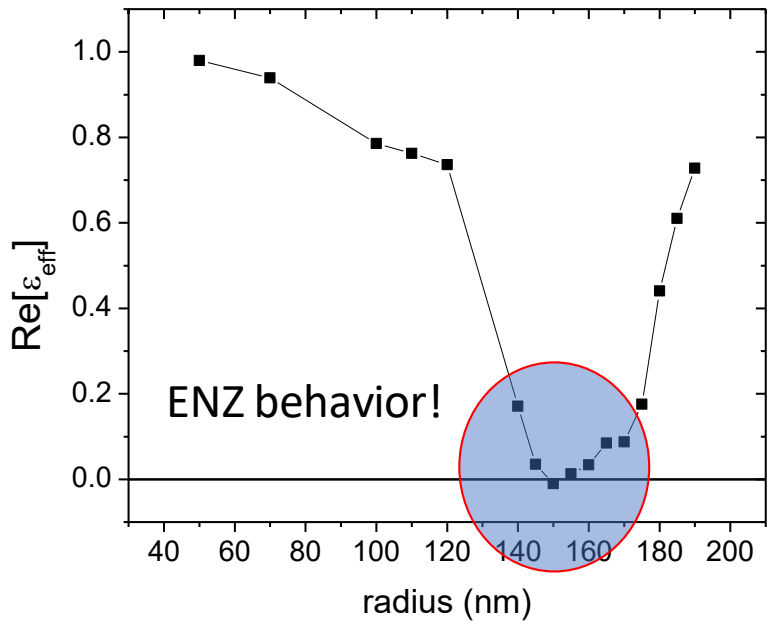

(d)

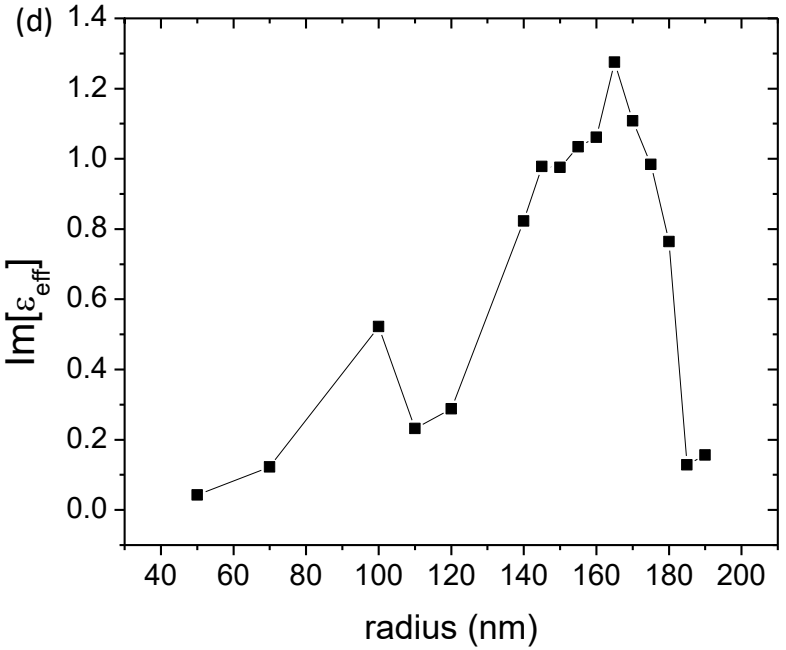

Analytical Homogenization of core-shell metamaterials: Mie Theory

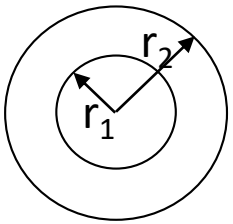

Validation of the theory

Simulations performed at BU

Mie-Lorenz coefficients (core-shell):

$$a_m = \frac{\psi_m(y)[\psi_m'(n_2 y) - A_m \chi_m'(n_2 y)] - n_2 \psi_m'(y)[\psi_m(n_2 y) - A_m \chi_m(n_2 y)]}{\xi_m(y)[\psi_m'(n_2 y) - A_m \chi_m'(n_2 y)] - n_2 \xi_m'(y)[\psi_m(n_2 y) - A_m \chi_m(n_2 y)]}$$

$$B_m = \frac{n_2 \psi_m(n_1 x)\psi_m'(n_2 x) - n_1 \psi_m(n_2 x)\psi_m'(n_1 x)}{n_2 \chi_m'(n_2 x)\psi_m(n_1 x) - n_1 \psi_m'(n_1 x)\chi_m(n_2 x)}$$

$$b_m = \frac{n_2 \psi_m(y)[\psi_m'(n_2 y) - B_m \chi_m'(n_2 y)] - \psi_m'(y)[\psi_m(n_2 y) - B_m \chi_m(n_2 y)]}{n_2 \xi_m(y)[\psi_m'(n_2 y) - B_m \chi_m'(n_2 y)] - \xi_m'(y)[\psi_m(n_2 y) - B_m \chi_m(n_2 y)]}$$

$$A_m = \frac{n_2 \psi_m(n_2 x)\psi_m'(n_1 x) - n_1 \psi_m'(n_2 x)\psi_m(n_1 x)}{n_2 \chi_m(n_2 x)\psi_m'(n_1 x) - n_1 \chi_m'(n_2 x)\psi_m(n_1 x)}$$

Homogenized bulk parameters:

$$\varepsilon_{eff} = \frac{k^3 + 4\pi i N a_1}{k^3 - 2\pi i N a_1}$$

$$\mu_{eff} = \frac{k^3 + 4\pi i N b_1}{k^3 - 2\pi i N b_1}$$

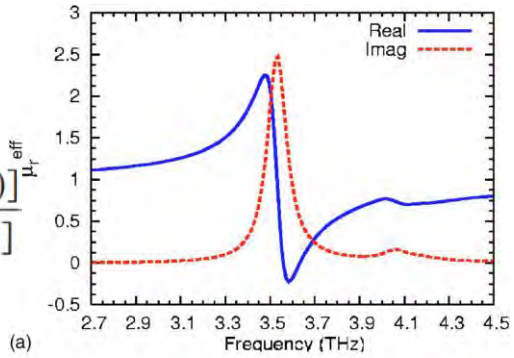

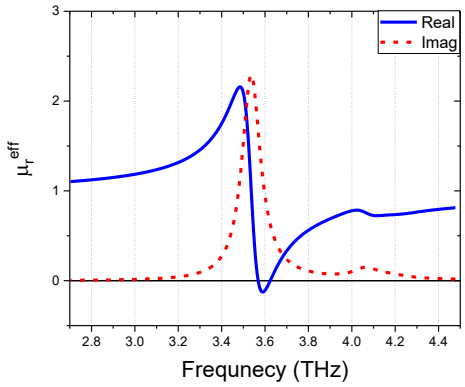

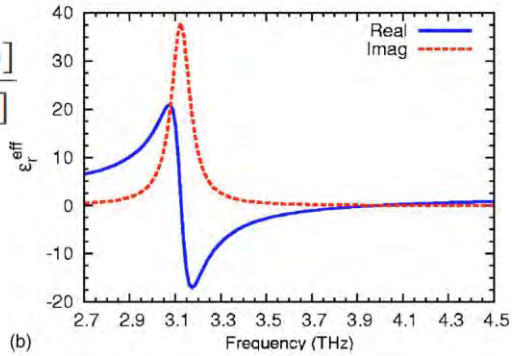

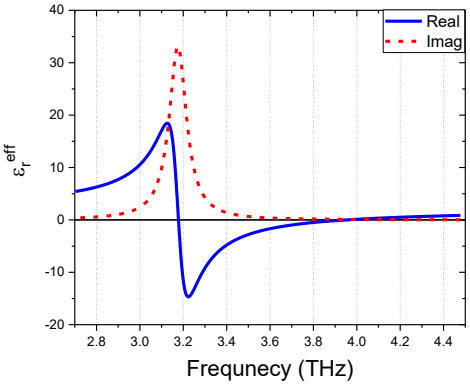

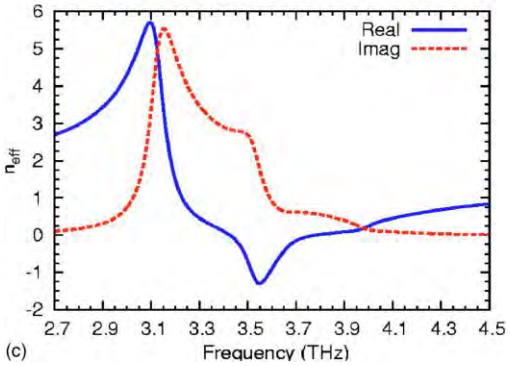

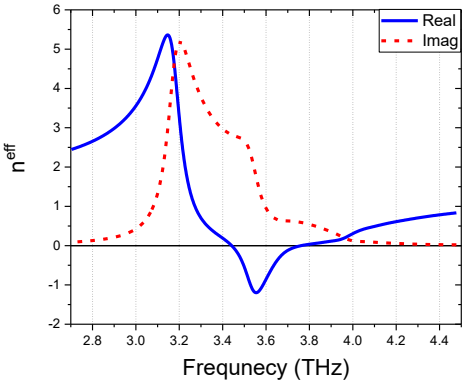

M. S. Wheeler, *et al.*, Phys. Rev. B 73, 045105 (2006)

Metamaterials parameters results with Si-ENZ nanoparticles

Effect of shell radius r_2

The white line indicates the contour of zero values

Fixed Si radius: r_1=140nm Filling fraction: 0.45 Drude ENZ model

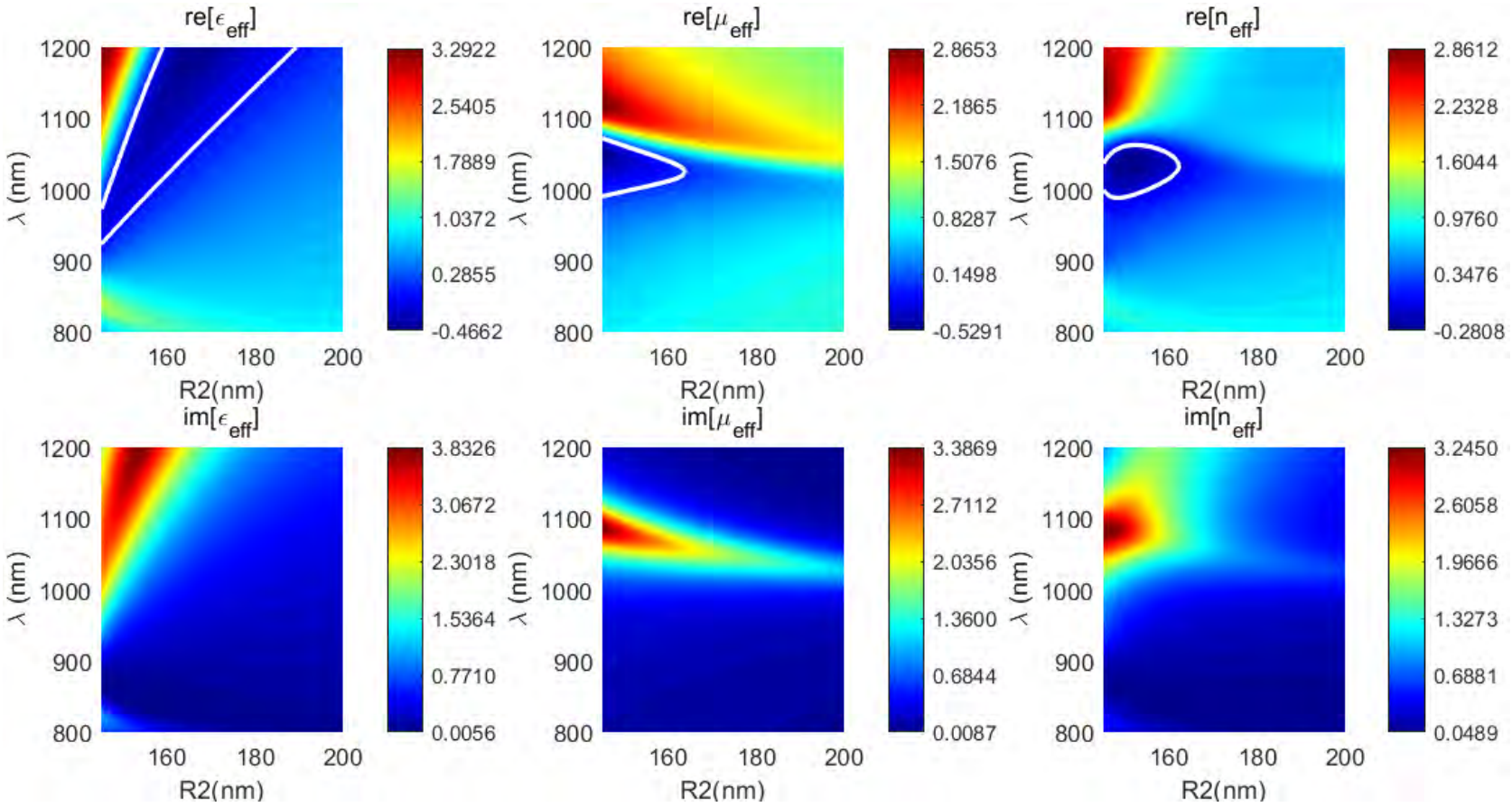

- We demonstrate doubly negative behavior in the near-IR by combining Si core with engineered plasmonic materials (ITO with tunable ENZ)!

Y. Wang, et al, "*Tunability of indium tin oxide materials for mid-infrared plasmonics applications*", **Opt. Mat. Express 7,** 2727 (2017)

Metamaterials parameters: effect of the ENZ wavelength

Fixed Si radius: r_1=140nm Fixed shell radius: r_2=155nm Filling fraction: 0.45 Drude ENZ model

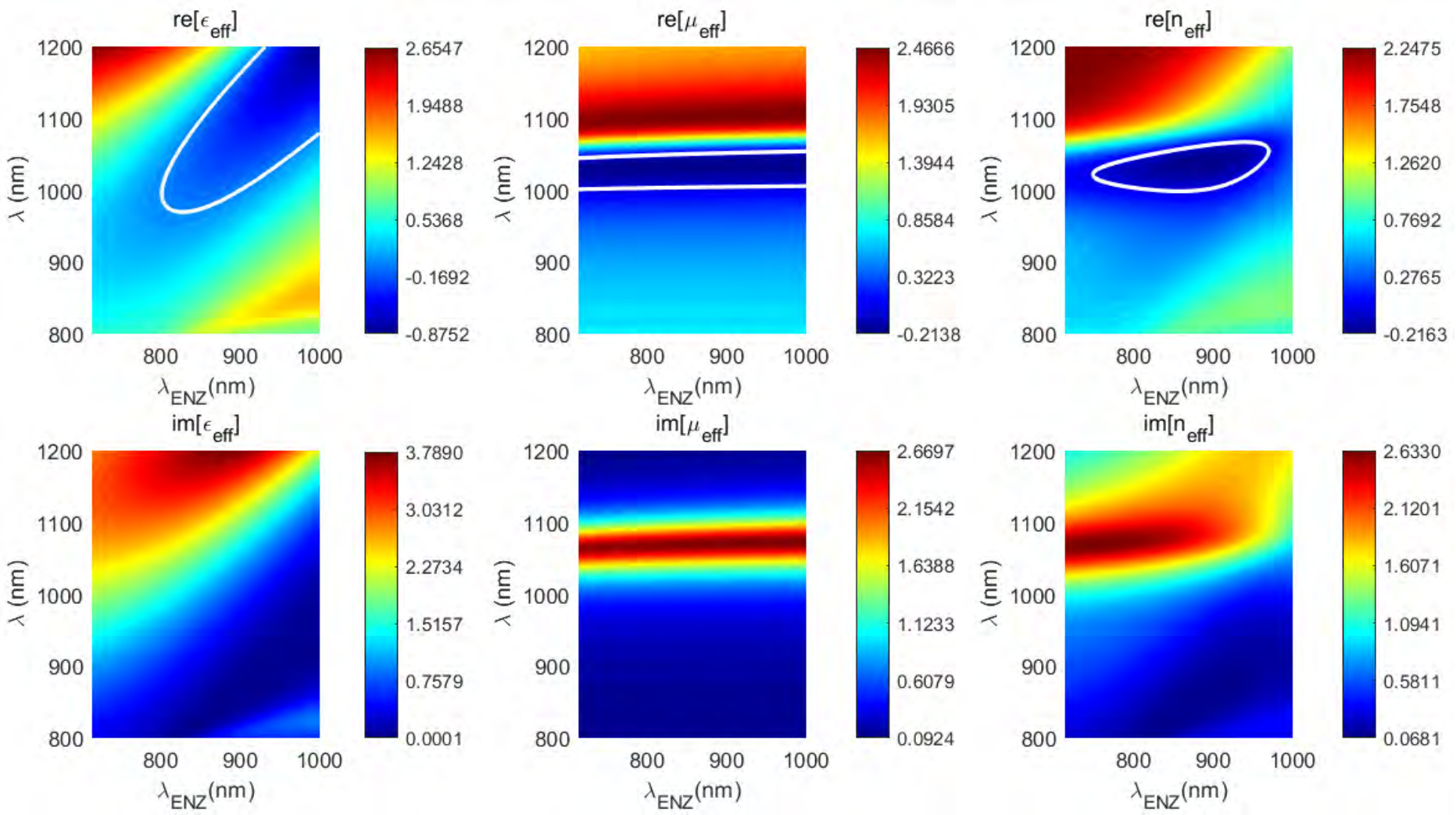

The white line indicates the contour of zero values

Metamaterials parameters: effect of finite ENZ losses

Fixed Si radius: r_1=140nm Fixed shell radius: r_2=155nm Filling fraction: 0.45 (Fixed plasma frequency)

$$\varepsilon(\omega)=\varepsilon_1(\omega)+i\varepsilon_2(\omega)=\varepsilon_\infty-\frac{\omega_p^2}{\omega^2+i\Gamma\omega}$$

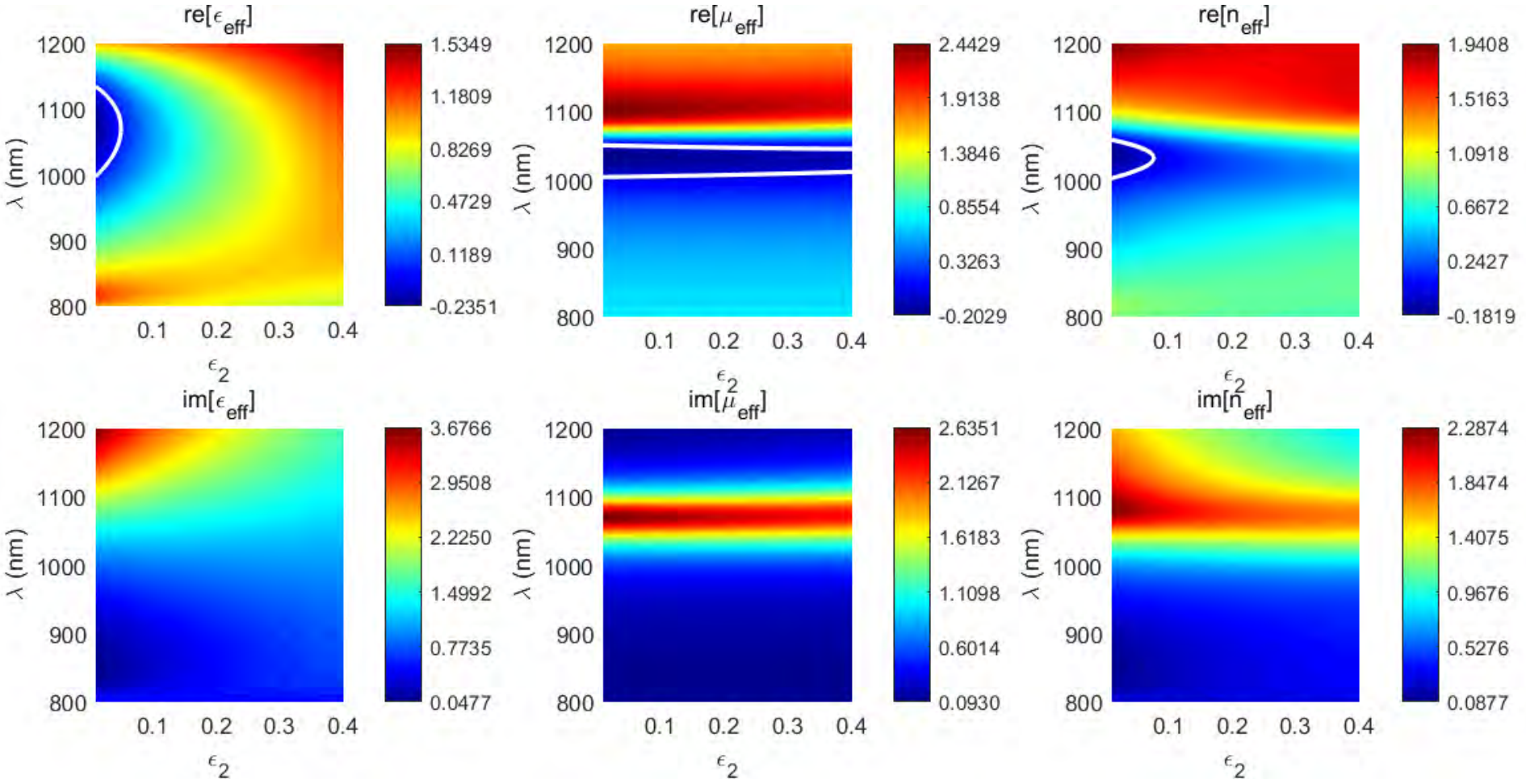

The white line indicates the contour of zero values

Nonlinear Homogenization with ENZ core-shell media

We studied enhancement of the nonlinear response of core-shell dielectric metamaterials

$$\chi_{eff}^{[3]} = f\left(\frac{3\varepsilon_h}{\varepsilon_{eff}+2\varepsilon_h - f(\varepsilon_{eff}-\varepsilon_h)}\right)^4 \chi^{[3]}$$

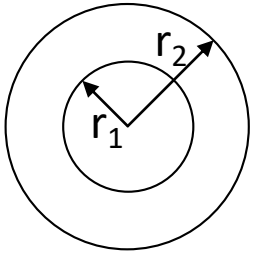

- 0<r<r1, Si, fixed r_1=140nm
- r1<r<r2, Drude metal
  ω p=3.4e14*2π rad/s
- Filling factor=0.45

Need to understand nonlinear homogenization beyond quasi-statics.
Very important topics, very little is known presently.

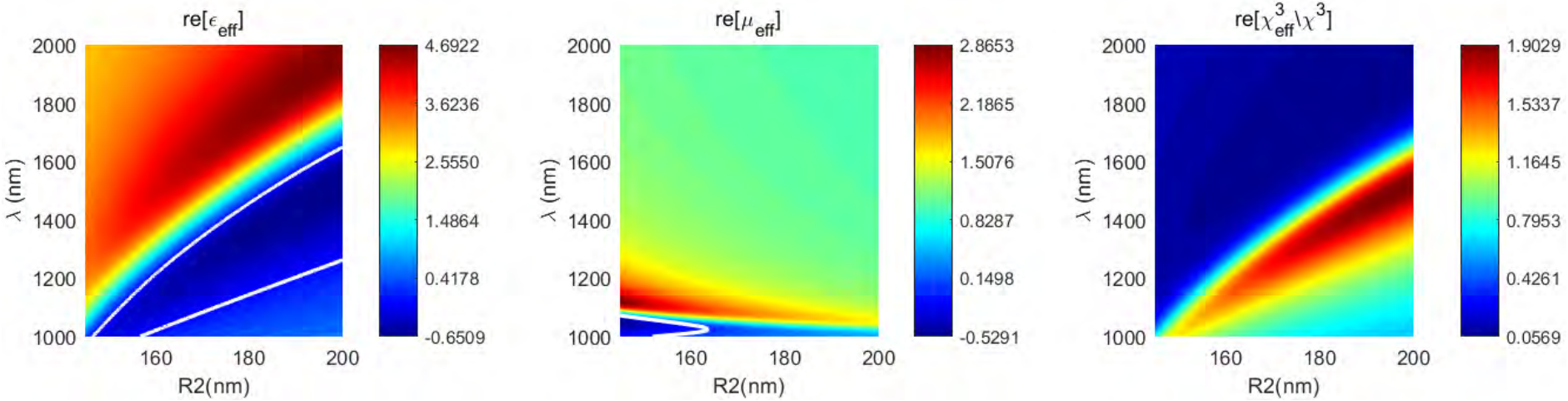

- Demonstrated potential to significantly enhance third-order nonlinearity in Si using core-shell homogenization approach with ENZ tunable plasmonic materials

Y. Wang, A. Capretti and L. Dal Negro, "*Wide tuning of the optical and structural properties of alternative plasmonic materials*", Opt. Mat. Express, 5, 2417 (2015).
Y. Wang, et al, "*Tunability of indium tin oxide materials for mid-infrared plasmonics applications*", **Opt. Mat. Express 7,** 2727 (2017)

A. Sihvola, Electromagnetic Mixing Formulas with Applications, IET (1999)

More general method: CPA homogenization of metamaterials

Basic Idea: zero out the T matrix of the inclusion with respect to the effective medium

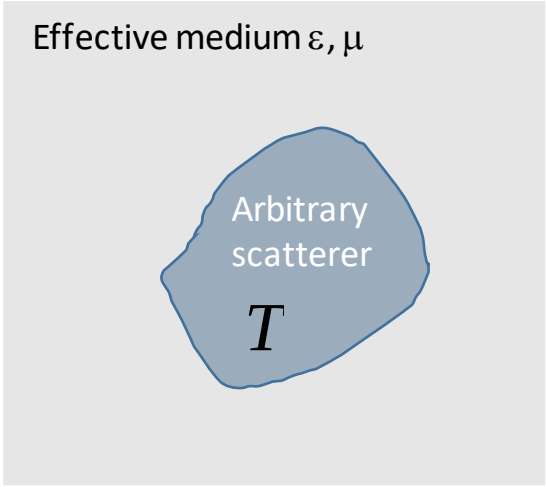

CPA Green's matrix:

$$\mathbf{G} = \mathbf{G}_e + \mathbf{G}_e \mathbf{T} \mathbf{G}_e$$

CPA condition:

$$\mathbf{T} = 0$$

→ Effective medium parameters ε, μ

Valid for any particles' morphology and beyond the quasi-static limit

P. Sheng, *Introduction to wave scattering, localization and mesoscopic phenomena*, Springer, 2006

CPA validation, canonical shapes (spheres) for ε

Example structure parameters:

- 0<r<r1 Drude metal
- r1<r<r2, air layer
- r2<r, effective medium

Case study: 3D array of Drude spheres

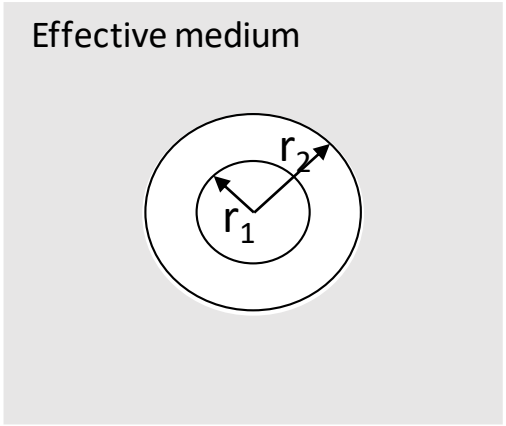

Effective permittivity of the metamaterial:

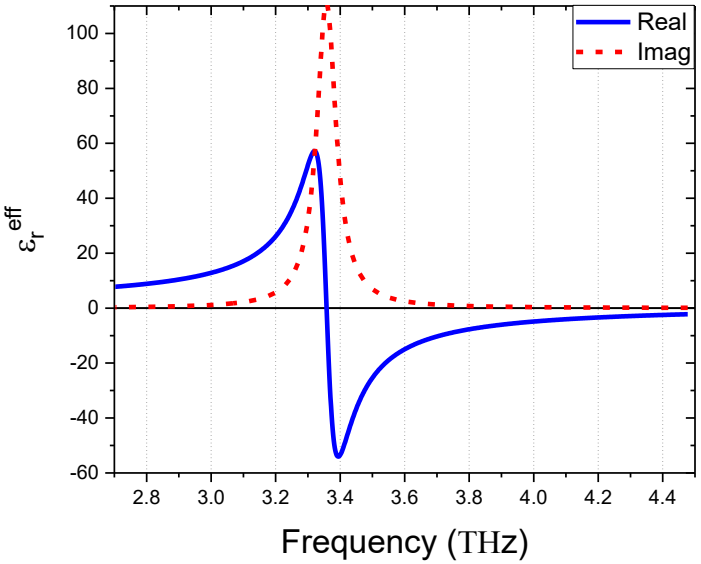

Mie-Lorentz coefficients:

$$a_1 = \frac{-k_1\mu_2\psi_1(k_1r_1)\psi_1'(k_2r_1) + k_2\mu_1\psi_1(k_2r_1)\psi_1'(k_1r_1)}{k_1\mu_2\psi_1(k_1r_1)\xi_1'(k_2r_1) - k_2\mu_1\xi_1(k_2r_1)\psi_1'(k_1r_1)}$$

$$b_1 = \frac{-k_2\mu_1\psi_1(k_1r_1)\psi_1'(k_2r_1) + k_1\mu_2\psi_1(k_2r_1)\psi_1'(k_1r_1)}{k_2\mu_1\psi_1(k_1r_1)\xi_1'(k_2r_1) - k_1\mu_2\xi_1(k_2r_1)\psi_1'(k_1r_1)}$$

Analytical homogenization result:

$$\varepsilon_{eff}^{r} = \frac{2[\psi_1(k_2r_2) + \xi_1(k_2r_2)a_1]}{k_2r_2[\psi_1'(k_2r_2) + \xi_1'(k_2r_2)a_1]}$$

Y. Wu et al., Phys. Rev. B 74, 085111 (2006)

CPA validation, canonical shapes (spheres) for μ

- 0<r<r1, LiTaO3
- r1<r<r2, air layer
- r2<r, effective medium

Effective magnetic permeability of the metamaterial:

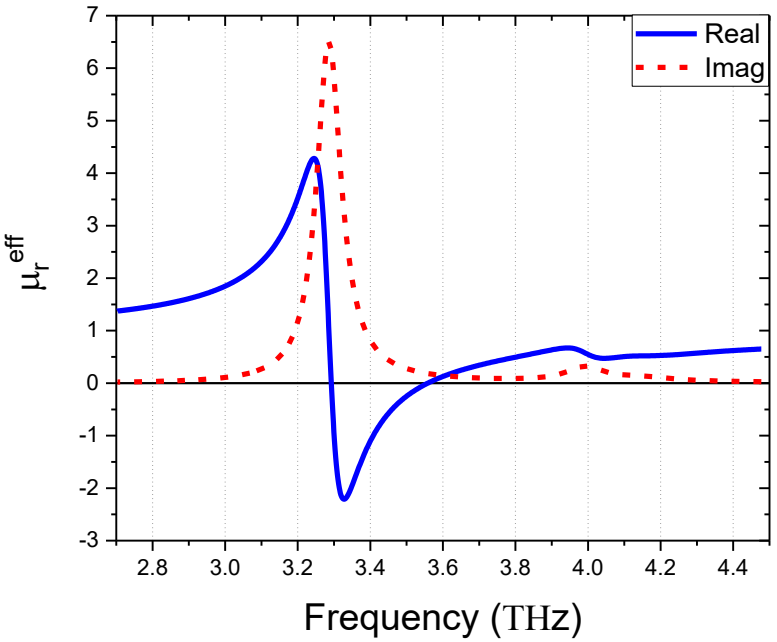

Analytical homogenization result:

$$\mu_{eff}^{r} = \frac{2[\psi_1(k_2 r_2) + \xi_1(k_2 r_2) b_1]}{k_2 r_2 [\psi_1'(k_2 r_2) + \xi_1'(k_2 r_2) b_1]}$$

Validation of Wu's CPA method

Ag using Drude model

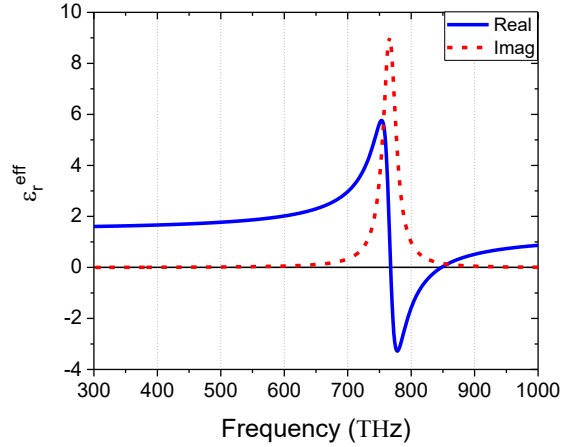

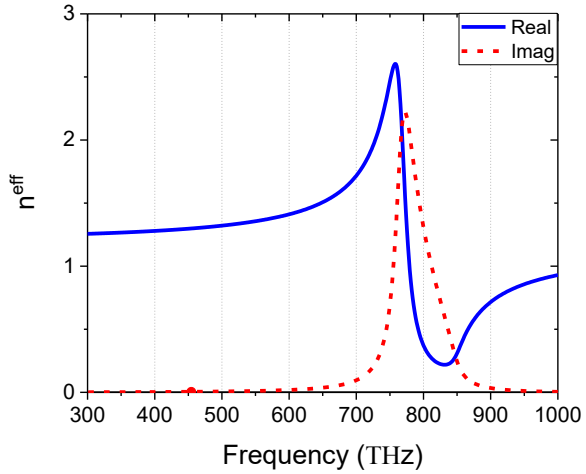

- 0<r<r1 r1<r<r2, air layer with $\frac{4\pi}{3} r_2^3 = a^3$
- r2<r, effective medium

Effective medium

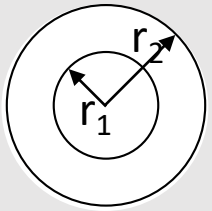

Ag using Johnson Christy dispersion data

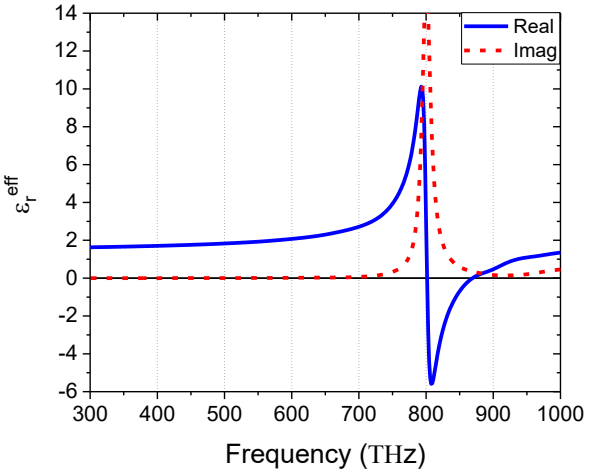

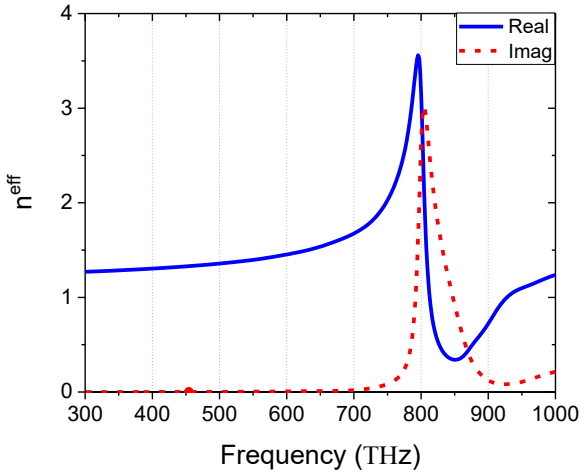

Mark S. Wheeler et. al. *Phys. Rev. B* , 73, 045105 (2006)

$$a_1 = \frac{k_1\mu_2\psi_1(k_1r_1)\psi_1'(k_2r_1) - k_2\mu_1\psi_1(k_2r_1)\psi_1'(k_2r_1)}{k_1\mu_2\psi_1(k_1r_1)\xi_1'(k_2r_1) - k_2\mu_1\xi_1(k_2r_1)\psi_1'(k_2r_1)}$$

$$b_1 = \frac{k_2\mu_1\psi_1(k_1r_1)\psi_1'(k_2r_1) - k_1\mu_2\psi_1(k_2r_1)\psi_1'(k_1r_1)}{k_2\mu_1\psi_1(k_1r_1)\xi_1'(k_2r_1) - k_1\mu_2\xi_1(k_2r_1)\psi_1'(k_1r_1)}$$

Y. Wu et. al. *Phys. Rev. B* , 74, 085111 (2006)

$$\varepsilon_{eff}^r = \frac{2(\psi_1(k_2r_2) - \xi_1(k_2r_2)a_1)}{k_2r_2(\psi_1'(k_2r_2) - \xi_1'(k_2r_2)a_1)}$$

$$\mu_{eff}^r = \frac{2(\psi_1(k_2r_2) - \xi_1(k_2r_2)b_1)}{k_2r_2(\psi_1'(k_2r_2) - \xi_1'(k_2r_2)b_1)}$$

Coupled Electric and Magnetic dipole Green's Matrix (EM-GM)

We developed an efficient Green's matrix code to model the EM response of arbitrary arrays of interacting nanoparticles with electric and magnetic dipole moments

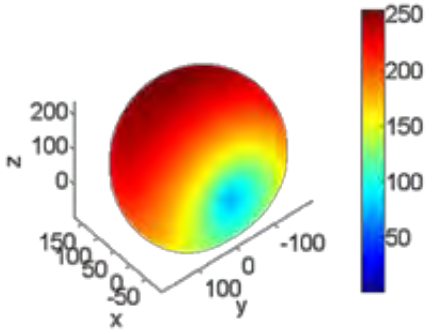

Total Green's matrix (6N X 6N) relating ***E*** and ***H*** fields: $G_{tot} = \begin{bmatrix} G_{ee} & G_{em} \\ G_{me} & G_{mm} \end{bmatrix}$

Standard 3 X 3 sub-block of diagonal blocks, G_{ee} and G_{mm}

$$G_{ee}^{\alpha\beta} = G_{mm}^{\alpha\beta} = (1-\delta_{\alpha\beta})\frac{3e^{ikr_{\alpha\beta}}}{2ikr_{\alpha\beta}}\left[\left(\frac{3}{k^2r_{\alpha\beta}^2}-\frac{3i}{kr_{\alpha\beta}}-1\right)\hat{r}_{\alpha\beta}\hat{r}_{\alpha\beta}+\left(1-\frac{1}{k^2r_{\alpha\beta}^2}-\frac{i}{kr_{\alpha\beta}}\right)I\right]$$

$$\hat{r}_{\alpha\beta} = r_{\alpha\beta}/|r_{\alpha\beta}|$$

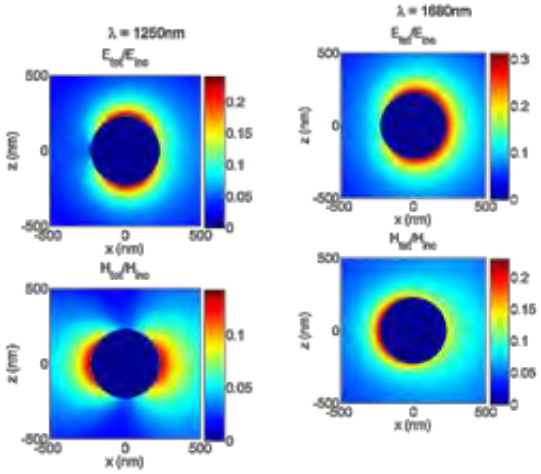

3 X 3 $\alpha\beta$-th sub-block in off-diagonal blocks, G_{me} and G_{em}:

$$G_{me}^{\alpha\beta} = -G_{em}^{\alpha\beta} = \frac{3e^{ikr_{\alpha\beta}}}{2ikr_{\alpha\beta}}\left(1+\frac{i}{kr_{\alpha\beta}}\right)\left(\frac{1}{|r_{\alpha\beta}|}\right)\begin{bmatrix} 0 & -r_{\alpha\beta}^{z} & r_{\alpha\beta}^{y} \\ r_{\alpha\beta}^{z} & 0 & -r_{\alpha\beta}^{x} \\ -r_{\alpha\beta}^{y} & r_{\alpha\beta}^{x} & 0 \end{bmatrix}$$

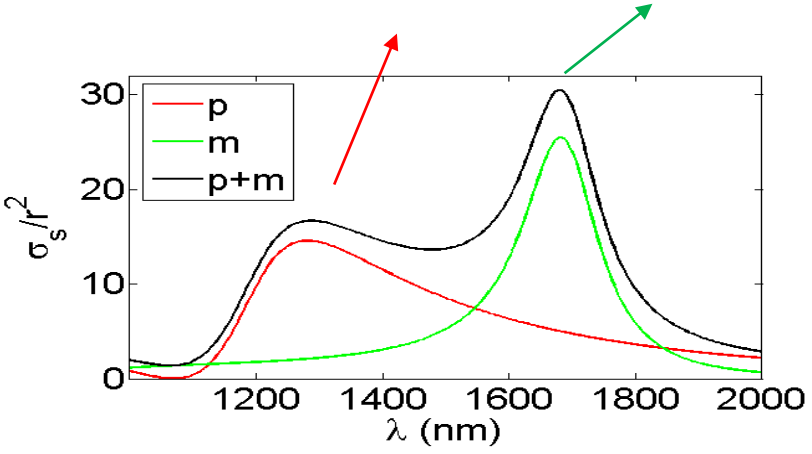

Mulholland et al, Lamgmuir, 10, 2533 (1994)
Sersic, et al., Phys. Rev. B, 83, 245102 (2011)

Photonic quasicrystals from complex primes

Primes in imaginary quadratic fields, quaternions and nanophotonics

- Study spectral statistics and wave localization in prime-based arrays.
- Engineering novel spectral properties in aperiodic scattering media.
- Discover novel diffraction phenomena in aperiodic optics.
- Demonstrating novel transport and localization effects.

$\mathbf{Z}[\omega] = \left\{ a + be^{2\pi i/3} : a, b \in \mathbf{Z} \right\}$ **Eisenstein prime array**

$\mathbf{Z}[i] = \left\{ a + b\sqrt{-1} : a, b \in \mathbf{Z} \right\}$ **Gaussian prime array**

Hurwitz prime array

Lifschitz prime array

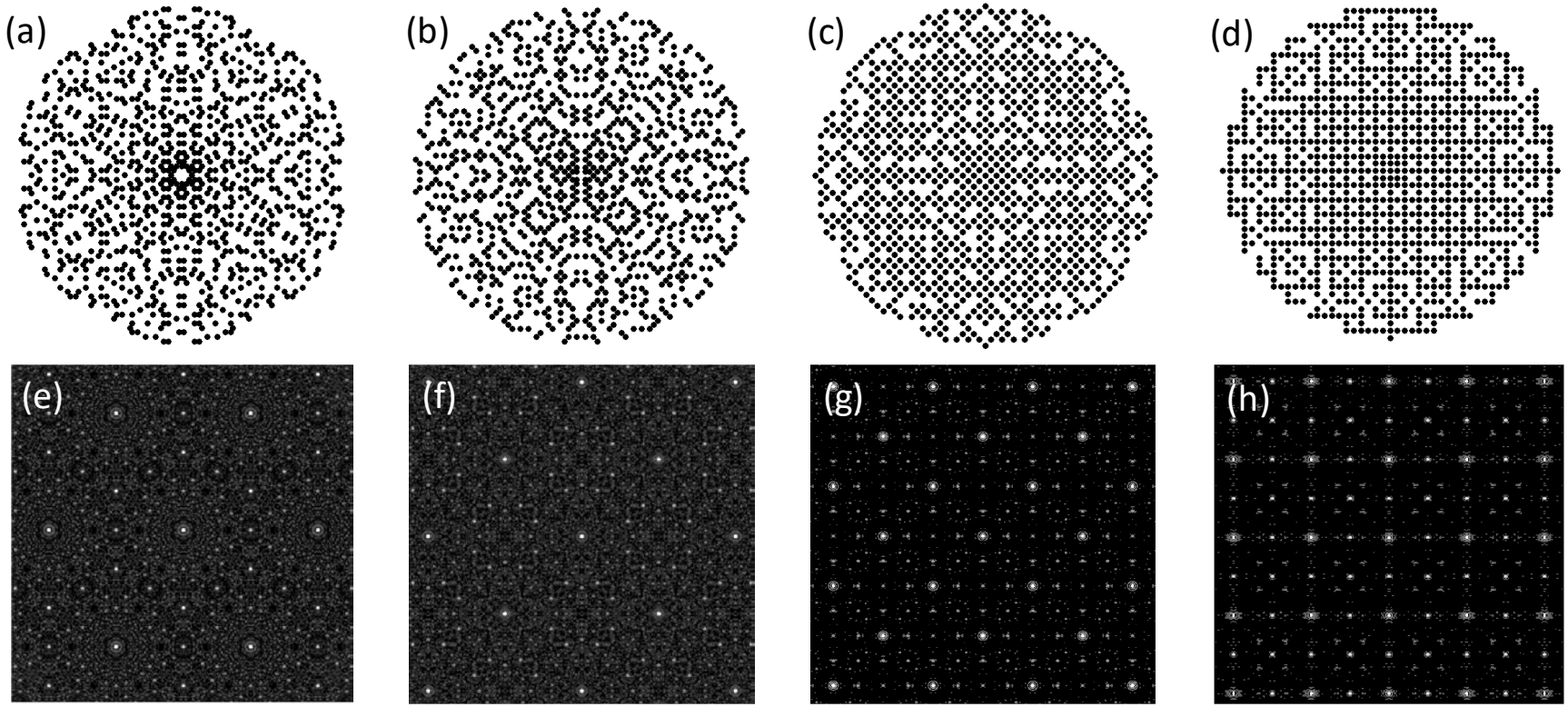

L. Dal Negro *et al*, Crystals 6, 161 (2016).

R. Wang, *et al*, Phys. Rev. B, 97, 024202 (2018).

Green' Matrix Method: spectral gaps via densities of states

DOS obtained by counting the number of eigenstates at each energies:

- Band gap creation at $\rho\lambda^2 \geq 10$; no bandgaps at lower densities.

Eisenstein prime array | **Gaussian prime array** | **Hurwitz prime array** | **Lifschitz prime array**

$\rho\lambda^2 = 100$

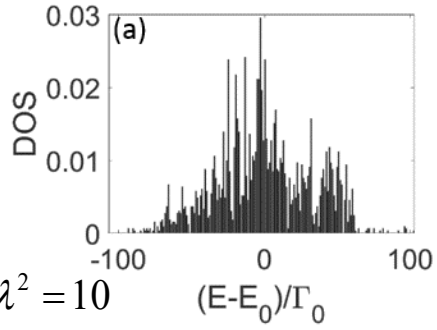

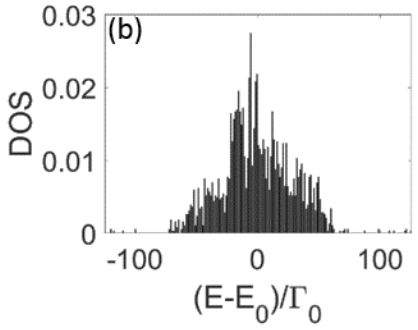

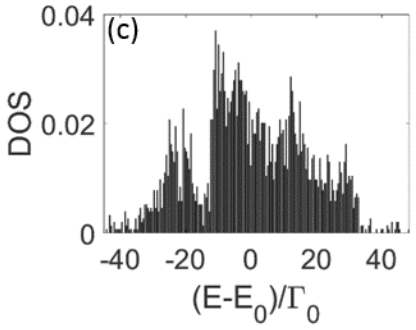

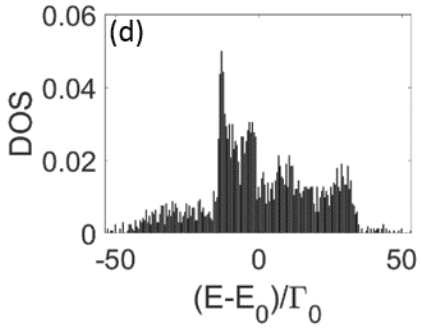

$\rho\lambda^2 = 10$

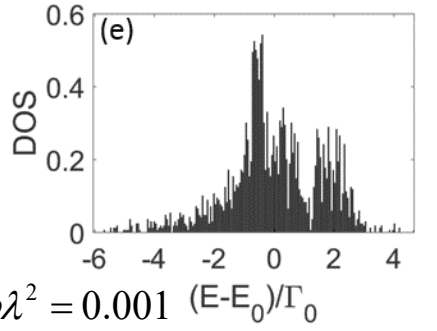

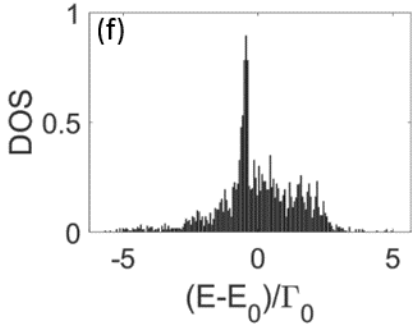

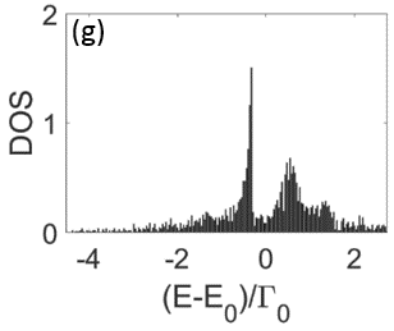

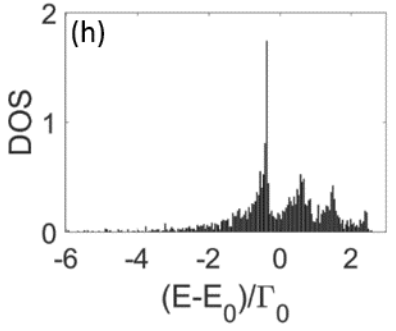

$\rho\lambda^2 = 0.001$

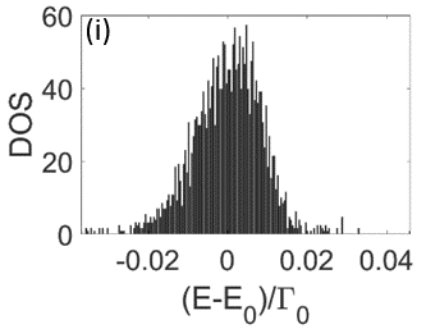

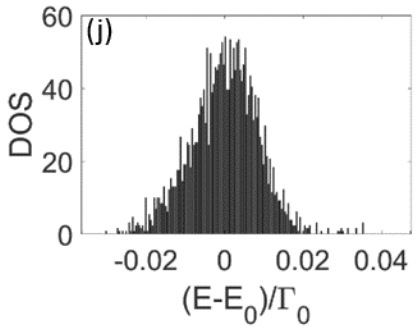

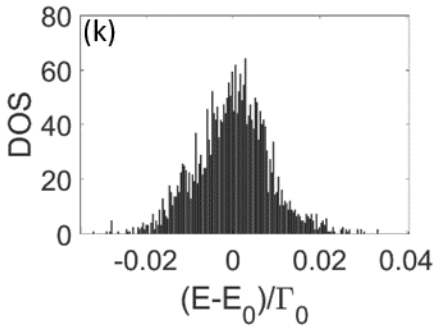

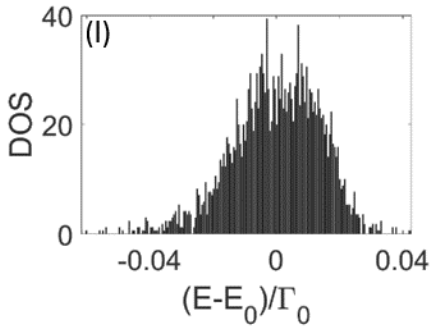

Spectral statistics: criticality and localization

Complex prime-based aperiodic systems: Level Statistics and Decay Rates

- Poisson level-spacing distribution in the localized regime ($\rho\lambda^2 = 100$);
- Critical distribution in the diffusive regime ($\rho\lambda^2 = 0.001$);
- Decay rate statistics shows the transition to light localization regime, similar to random systems;
- First observation of critical level statistics in aperiodically ordered media;
- Algebraic decay of $P(\Gamma)$ implies Anderson localization in opened media;

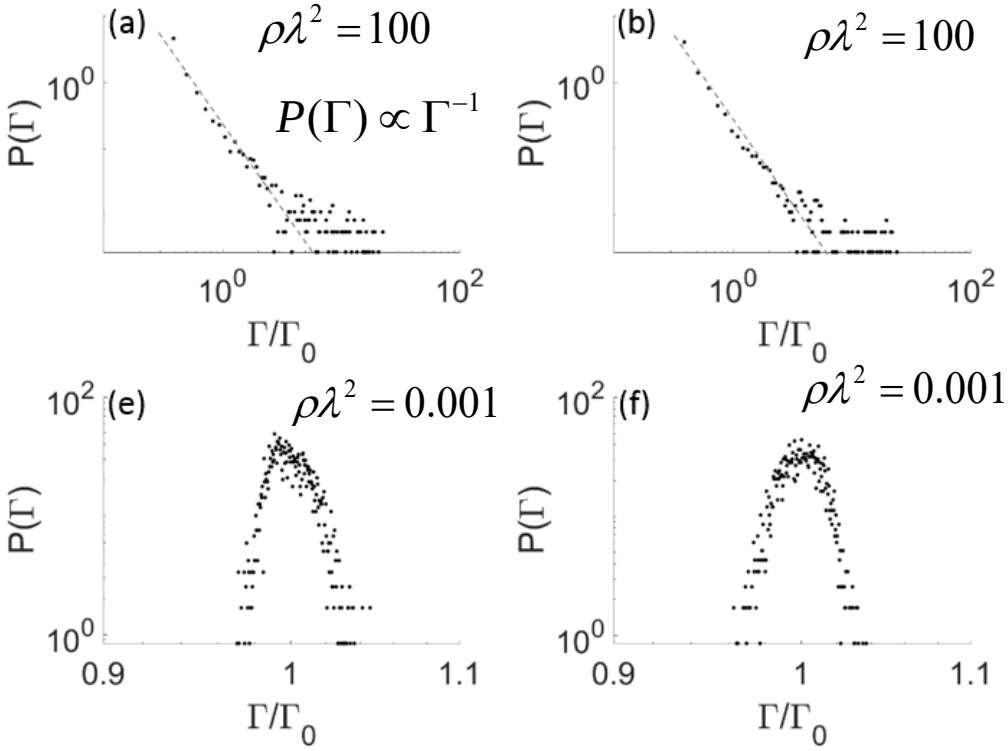

Poisson statistics: localization

$$P(s) \propto e^{-s}$$ no level repulsion

Critical statistics:

$$P(s) = \exp[\mu - \sqrt{\mu^2 + (A_c s)^2}]$$

Wigner surmise: diffusion

$$P(s) \propto \frac{\pi s}{2} e^{-\pi s^2/4}$$

R. Wang, *et al*, Phys. Rev. B, 97, 024202 (2018).

I. Zharekeshev, *et al*, Phys. Rev. Lett, 79, 717 (1997).

Comparison of mode localization in aperiodic arrays

Localization of eigenstates through IPR:

- max. IPR values at each optical densities for aperiodic arrays are bounded by random and periodic arrays;

- The highest IPR states in aperiodic structures are Efimov-type resonances localized on small clusters of particles;

$$IPR(\lambda_k) = \frac{\sum_n |e_n(\omega_k)|^4}{\sum_n |e_n(\omega_k)|^2}$$

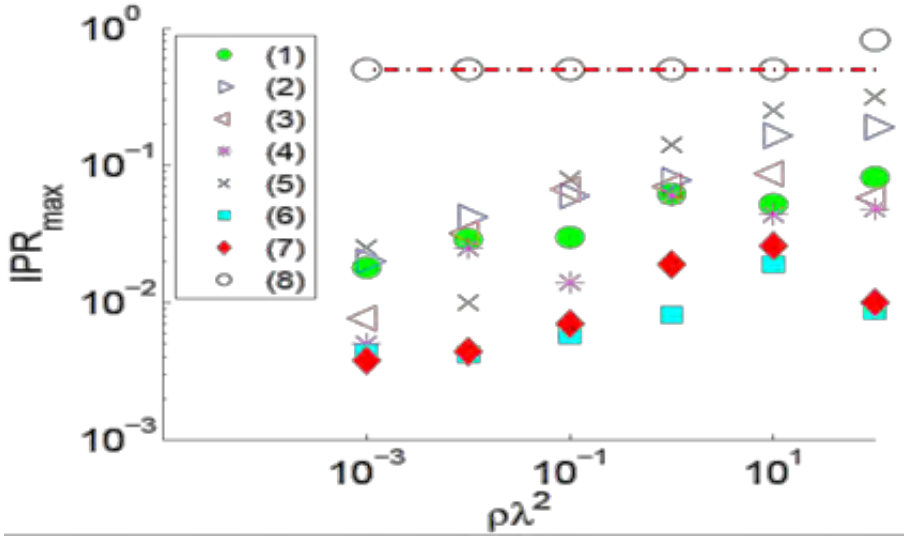

(1) Eisenstein prime, (2) Gaussian prime, (3) Lifschitz prime, (4) Hurwitz prime arrays, (5) Penrose, (6) square, (7) triangular and (8) uniform random arrays

$\rho\lambda^2 = 100$

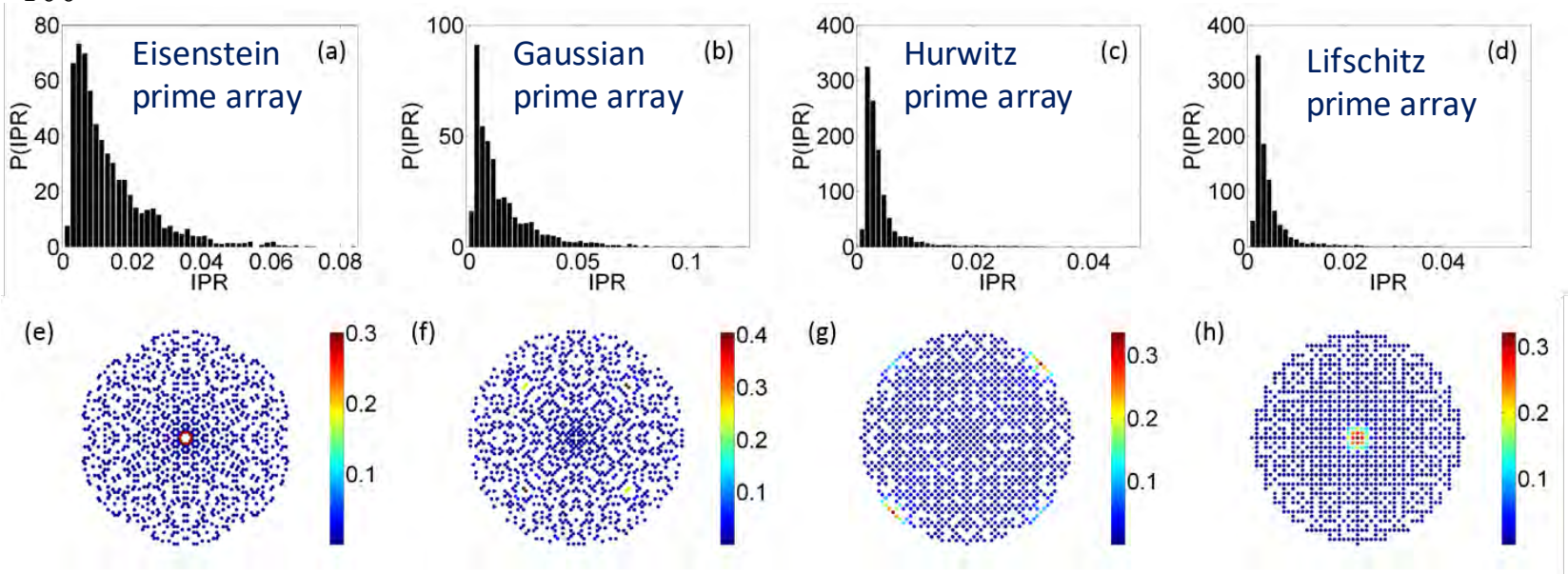

Complex Primes Arrays: TiO_2 nanoparticles @BU

Eisenstein prime array

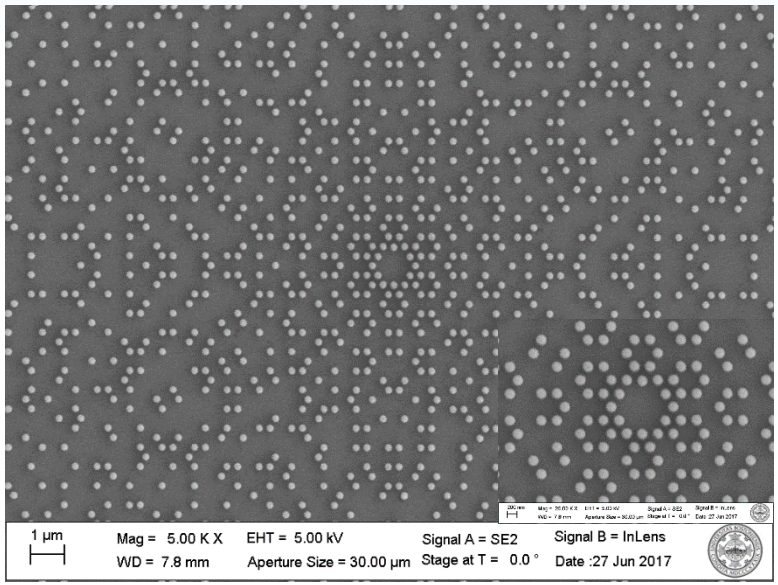

Gaussian prime array

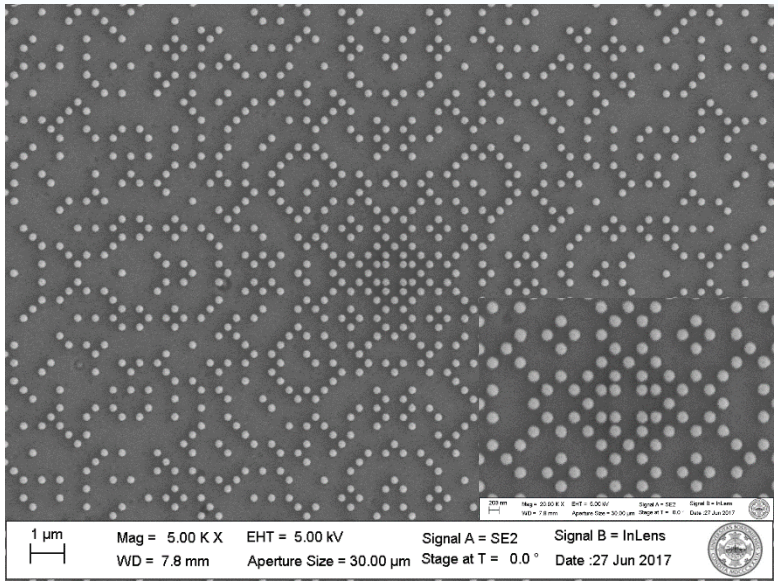

Hurwitz prime array

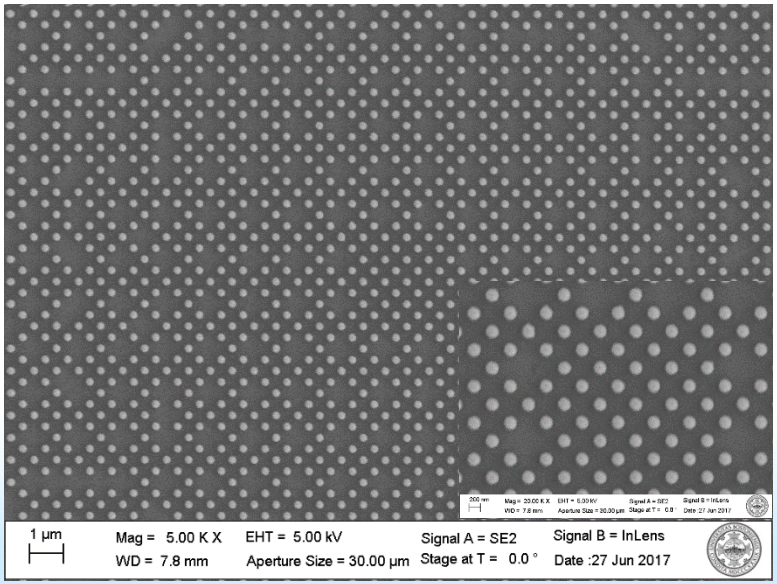

Lifschitz prime array

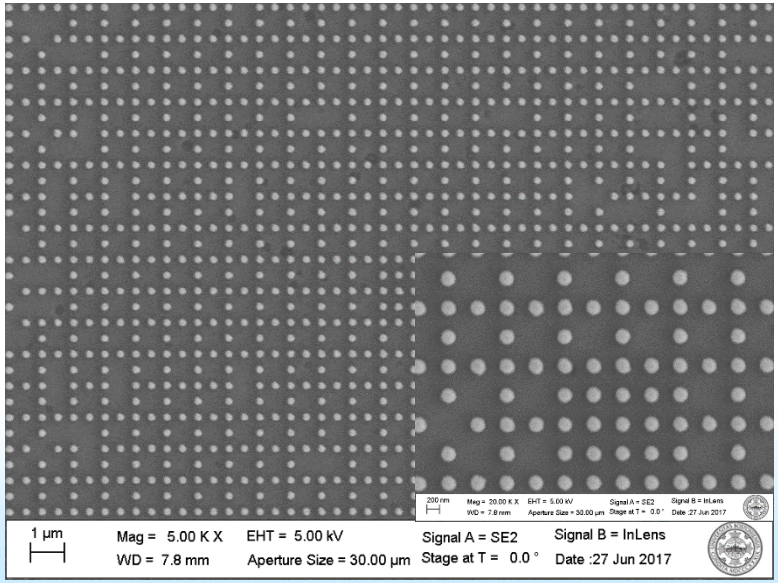

EM-Green's Matrix: Representative Eigenmodes of Eisenstein Prime

N ~ 1000 Eisenstein prime
Average separation = 550nm, wavelength = 600nm

Representative mode 1

Extended fractal mode 1

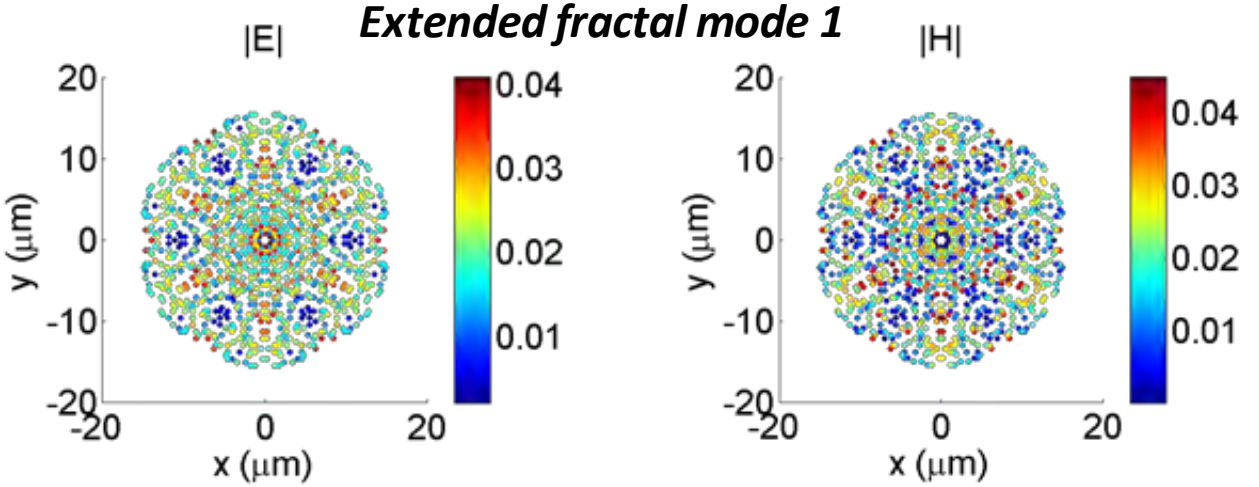

Representative mode 2

Extended fractal mode 2

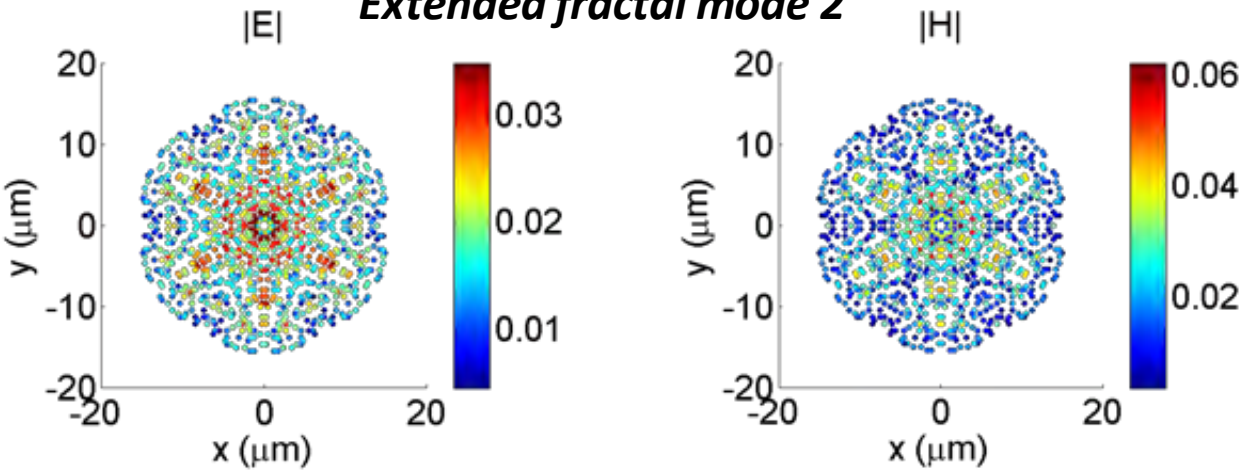

EM-Green's Matrix: Representative Eigenmodes of Eisenstein Prime

N ~ 1000 Eisenstein prime
Average separation = 550nm, wavelength = 600nm

Representative mode 3

Localized mode at the center

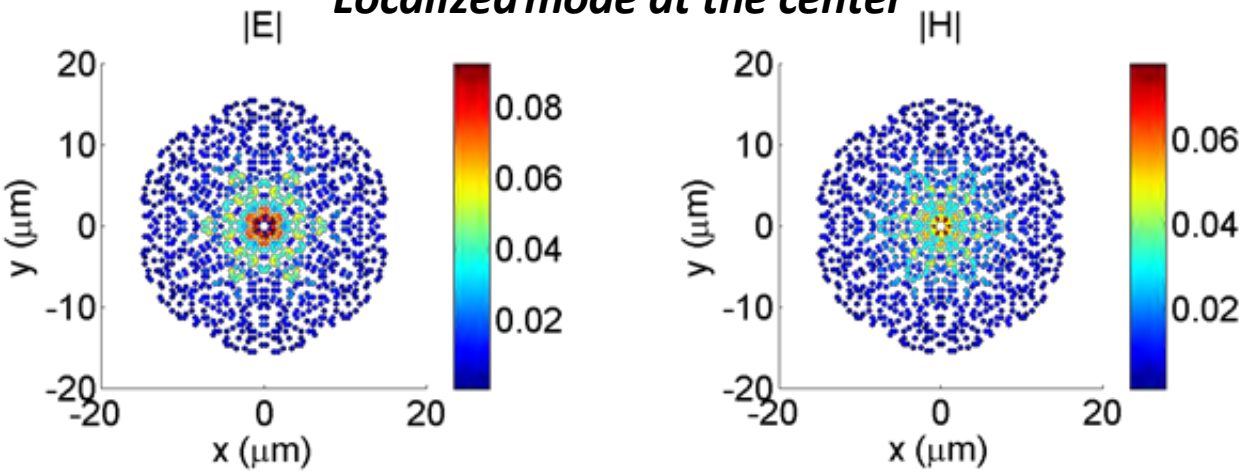

Representative mode 4

Concentric-ring modes

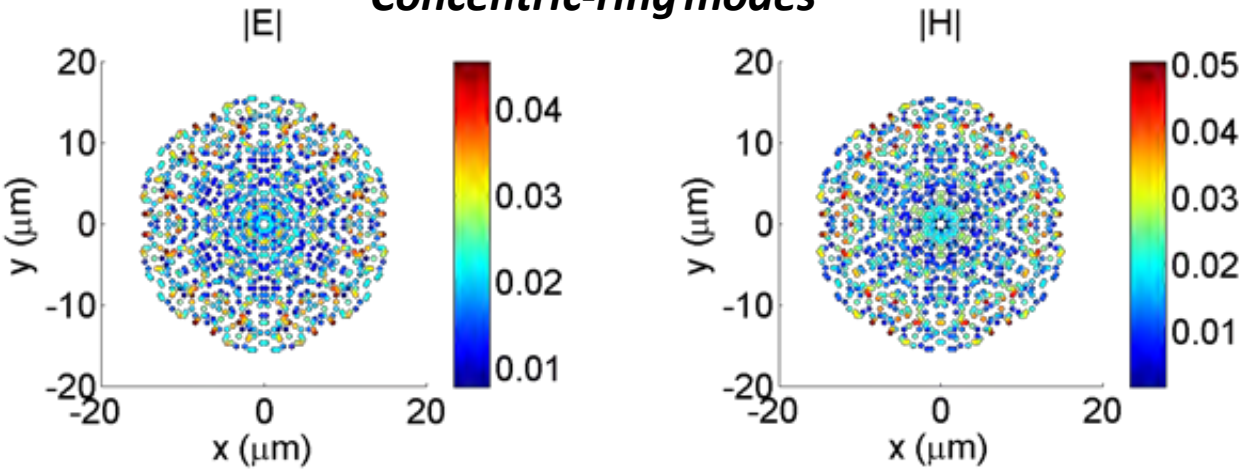

Measured Scattering Resonances of Eisenstein Prime Arrays

In collaboration with the Center for Nanoscale Systems, Harvard University

Overall array diameter 0.5mm, particle diameter = 200nm

Direct imaging of scattering resonances via multispectral dark-field spectroscopy

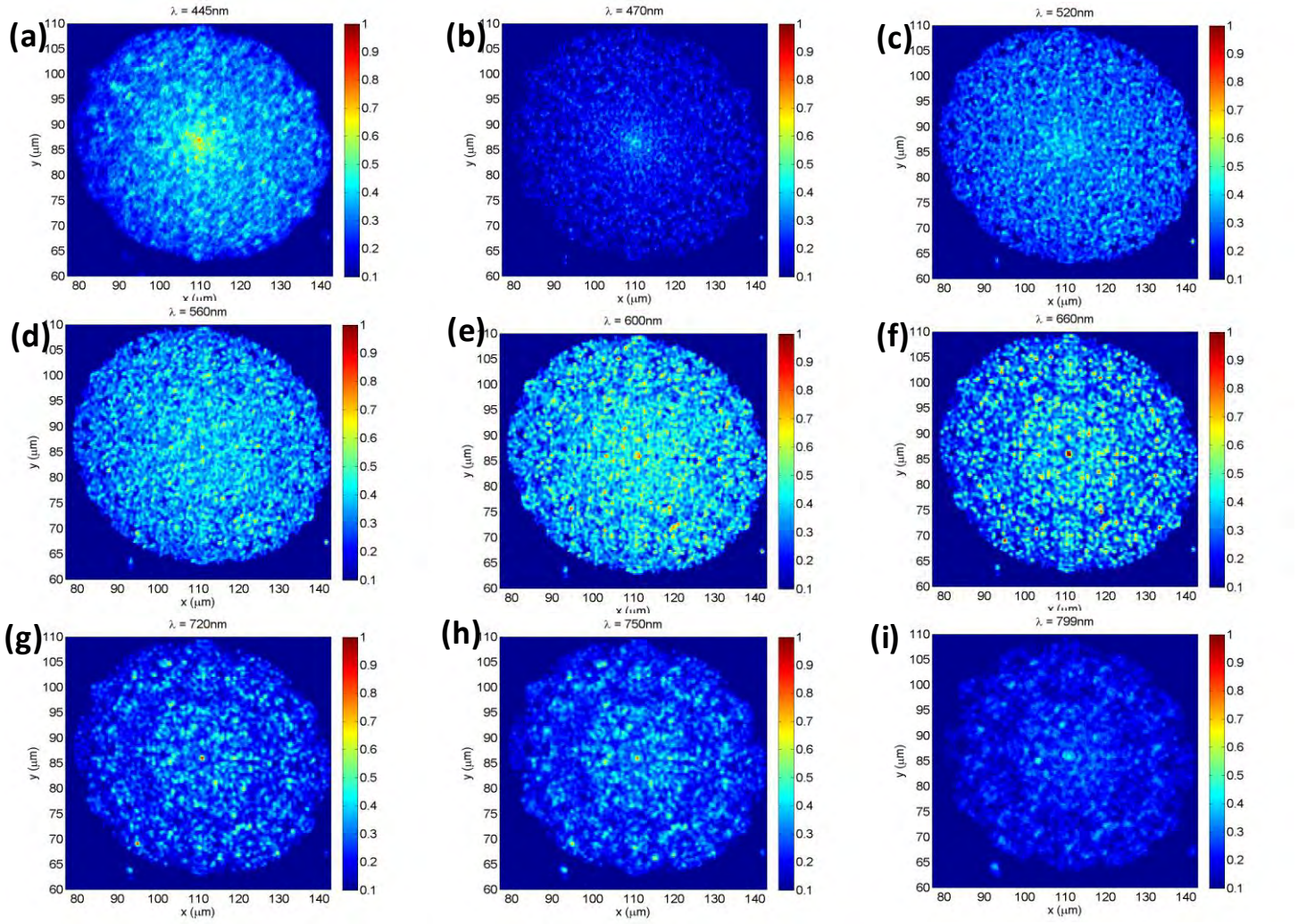

Eisenstein Prime: Experimental wavelength sweep - Intensity Distribution

In collaboration with the Center for Nanoscale Systems, Harvard University

Direct imaging of scattering resonances via multispectral dark-field spectroscopy

Experimental data

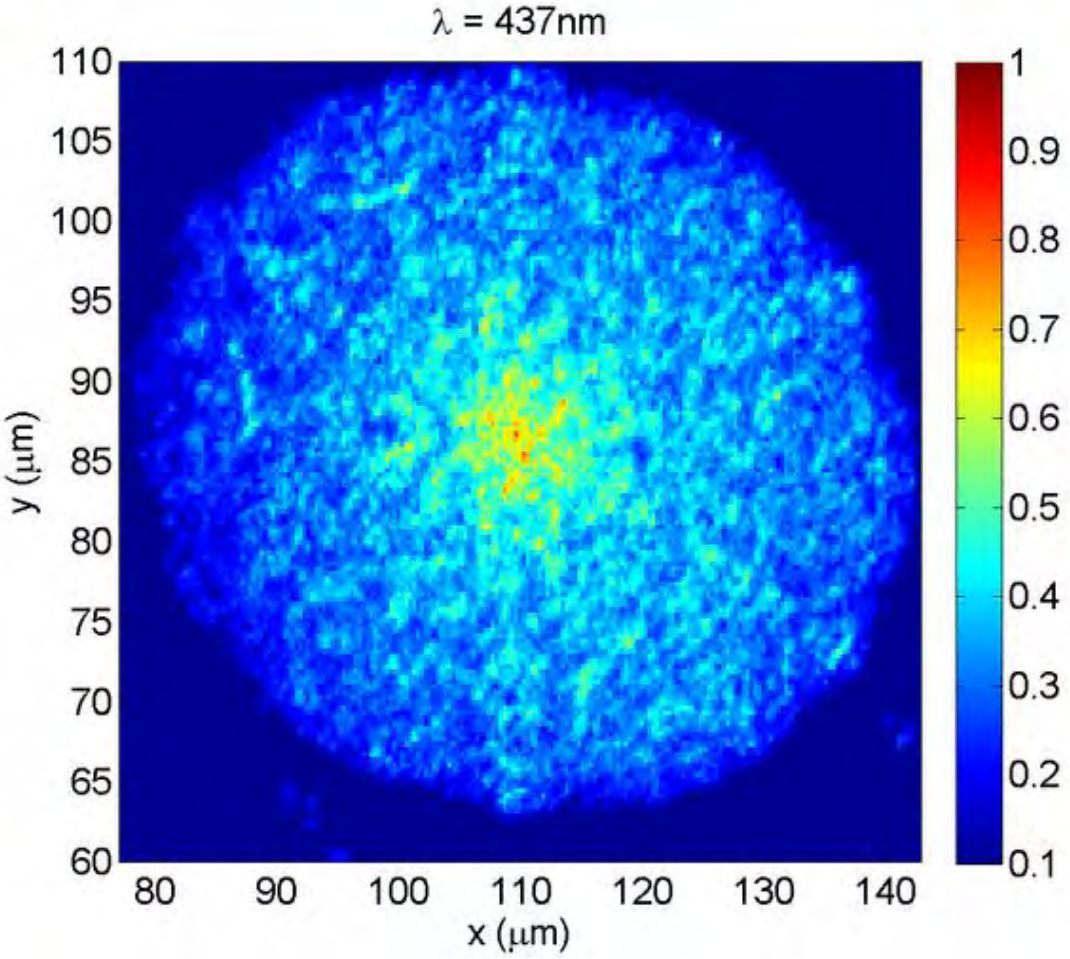

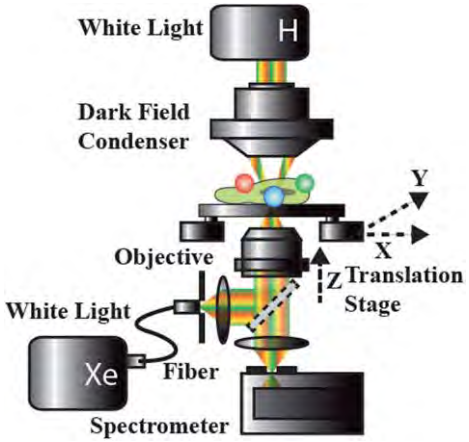

Stealth Hyper-uniform Systems: $S(k) \to 0$ as $k \to 0$

Example: engineering structural correlations through hyper-uniformity / Far-field

Weak correlations — **Strong**

X = 0.1

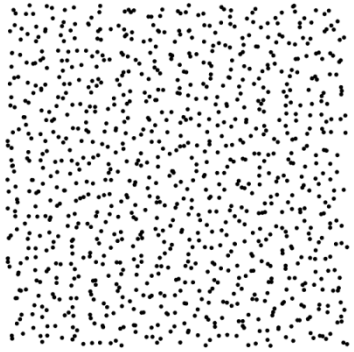

X = 0.3

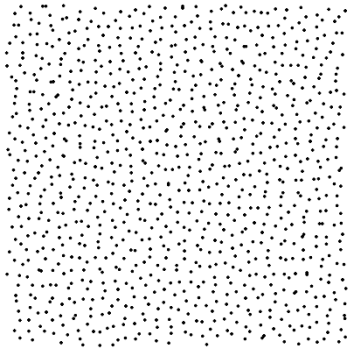

X = 0.6

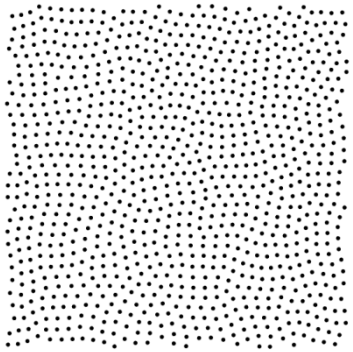

X = 0.9

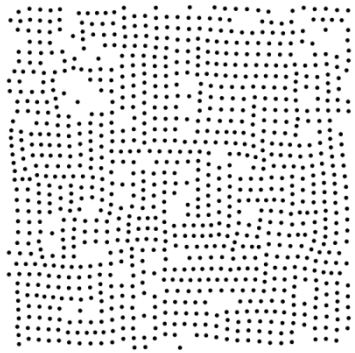

Radiation Diagrams / Structure Factors S(k)

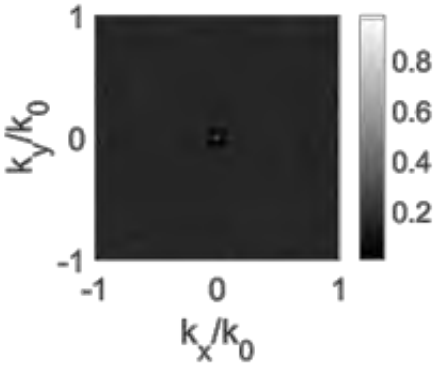

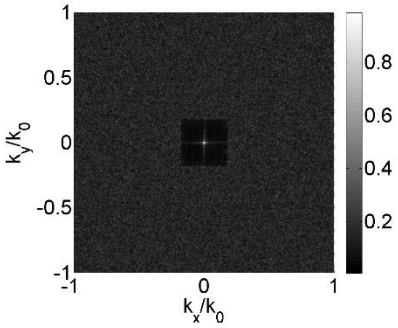

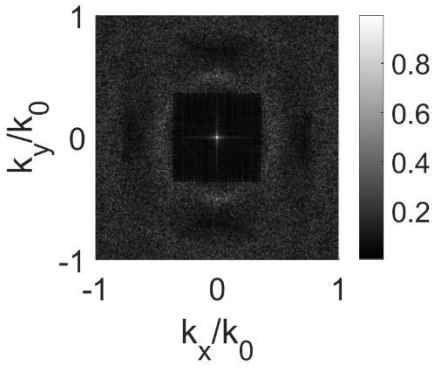

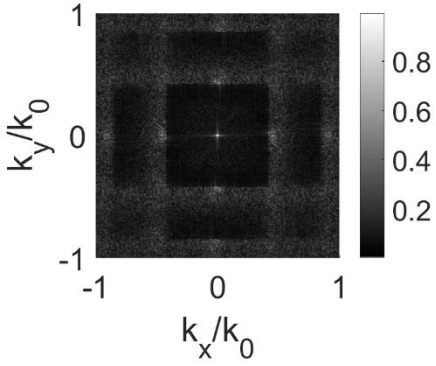

O. Leseur, et al., Optica 3, 763-767 (2016).

R. D. Batten, et al., J. Appl. Phys. 104, 033504 (2008).

State of the Art in Structured Diffraction

Vogel Spiral Points

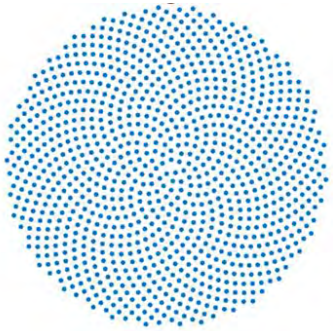

Stealth Hyperuniform Points

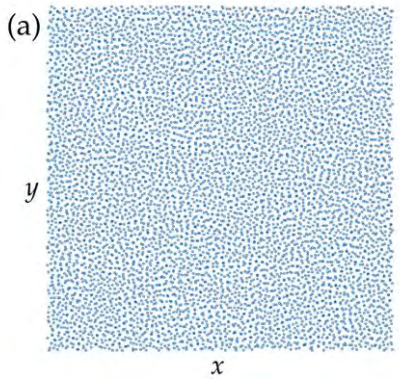

Diffraction Pattern

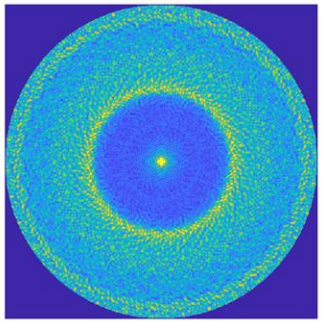

Diffraction Pattern

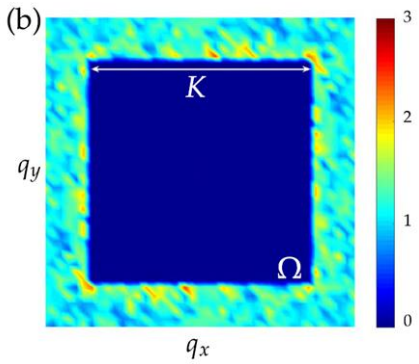

- Vogel Spiral (left)
  - deterministic pattern
  - circular exclusion in k-space (cone in real space) with power density enhancement in a ring around the exclusion
- Hyperuniform patterns (right)
  - Non-deterministic; created using optimization techniques
  - square exclusion in k-space
- Both patterns demonstrate potential for selective directional enhancement or nullification of scattered radiation

K. Guo, M. Du, C. I. Osorio, A. F. Koenderink, Laser & Photonics Reviews 2017, 11, 1600235

O. Leseur, R. Pierrat, and R. Carminati, "High-density hyperuniform materials can be transparent," Optica 3, 763-767 (2016)

Beyond Hyperuniformity: arbitrary targets in k-Space

Developed a simple algorithm to design arbitrary k-space in one-level diffracting structures

Significant Equations

Structure Factor
(far-field diffraction pattern)

$$S\left(\vec{k}\right) = |\mathcal{F}(P_i)|^2 = \frac{1}{N}\left|\sum_{j=1}^{N} e^{i\vec{k}\cdot\vec{r}_j}\right|^2$$

Potential function
(distance to target, S_o)

$$\Phi(\vec{r_1}, \ldots, \vec{r_N}) = \sum_{k\epsilon\Omega}[S(\vec{k}) - S_o(\vec{k})]^2$$

Potential Minimization

$$\underset{\vec{r_1}, \ldots \vec{r_N}}{argmin}\ \Phi(\vec{r_1}, \ldots, \vec{r_N})$$

Stealth Hyperuniform

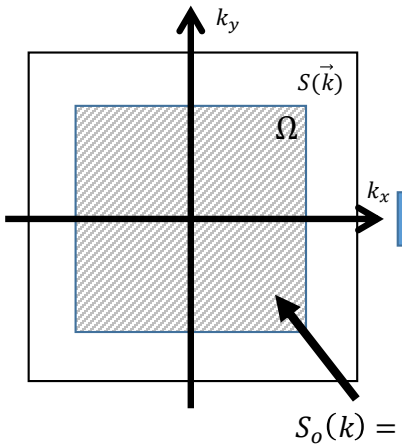

Arbitrary target shapes and non-zero target values

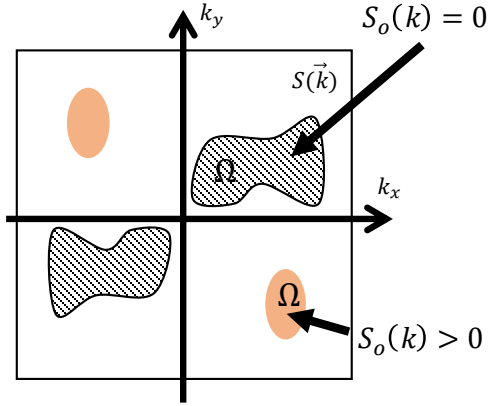

- Generate point patterns with target structure factor $S_o(\vec{k})$ by applying gradient descent method to Φ
- Current literature focuses on square or circular exclusions ($S_o = 0$), about $\vec{k} = 0$ (i.e. Stealth Hyperuniform patterns)
- We generate patterns with arbitrarily shaped exclusion and enhancement ($S_o > 0$) regions
  - No constraints on shape or continuity of target regions

S. Gorsky and L. Dal Negro (in preparation).

Enhancement of Vogel Spiral Diffraction

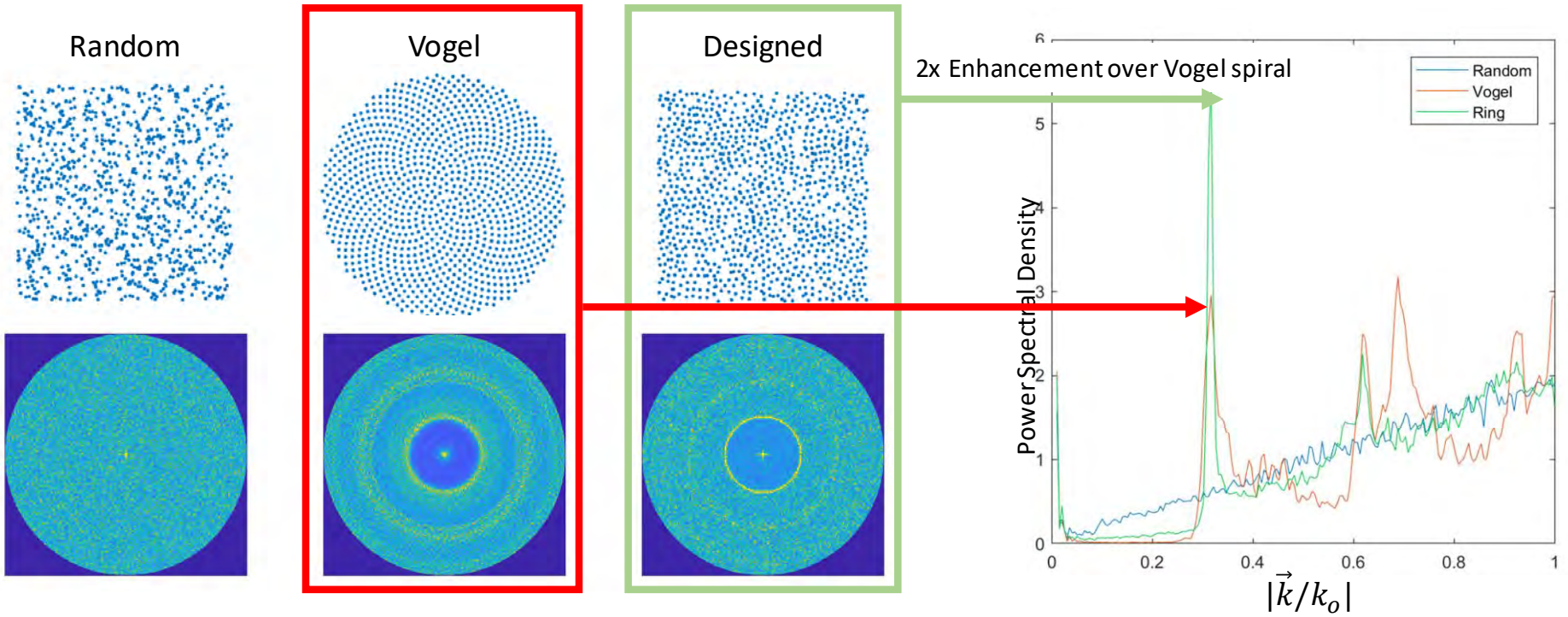

- Used optimization method to target structure factor with central exclusion and enhancement in the ring surrounding the exclusion
  - Designed pattern shows desired features (green boxed figure)
  - Bright ring has 2x power density enhancement compared to Vogel spiral

Can generate diffractive patterns with enhanced power spectral density in arbitrary directions and encode optical information in far-field (imaging, security, processing applications)

Arbitrary k-space Control: Target Exclusion Region

Particle Positions

Diffraction Patterns

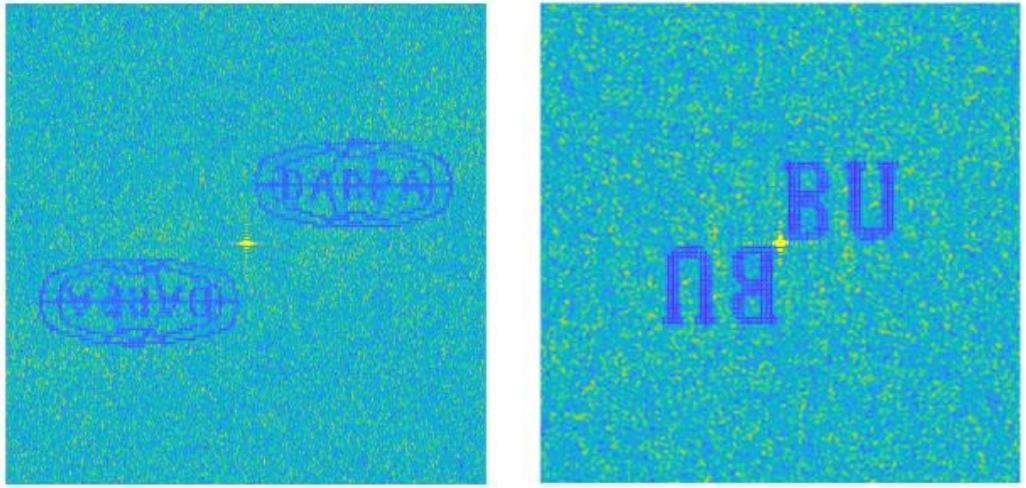

- Can generate unique diffractive radiation patterns
- No restrictions on shape or continuity of target regions
  - Except: Diffraction pattern will always be centrosymmetric

Robustness against Disorder

- Test stability of diffraction patterns by adding Gaussian noise to point positions
- *'a'* is the mean nearest neighbor separation

$$x_i \rightarrow x_i + \Delta x_i$$

$$y_I \rightarrow y_i + \Delta y_i$$

$$P(\Delta x) = P(\Delta y) = e^{-\Delta x^2/2\sigma}$$

(x_i, y_i)

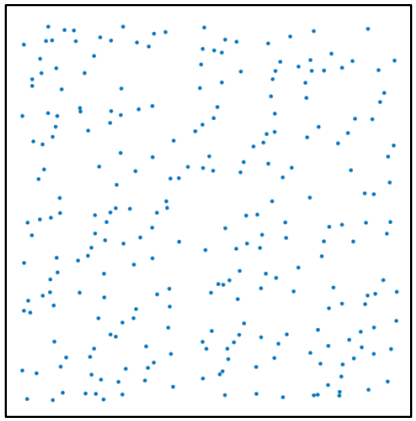

$\sigma = a/20$

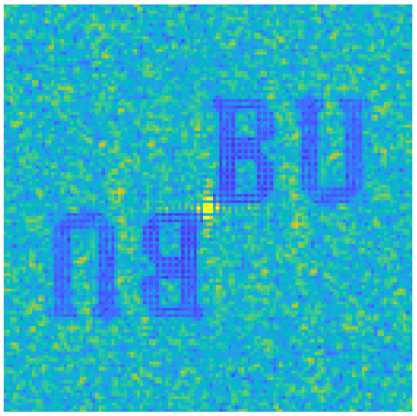

$\sigma = a/10$

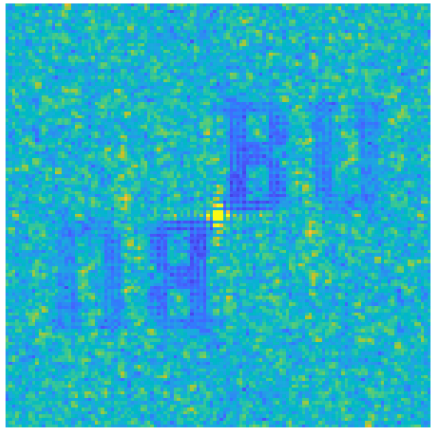

$\sigma = a/5$

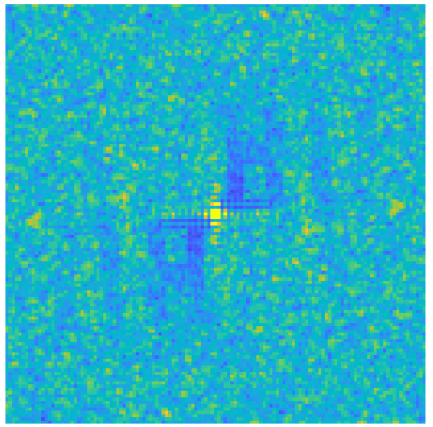

Diffraction pattern are stable down to standard deviation position error of $\sigma = a/10$

Wave Transport in "Colored Metamaterials"

Engineering light-matter interaction with structural correlations in non-periodic media

- Understanding the role of structural correlations to control light propagation
- Predicting dark and radiative states in complex nanoparticle arrays of arbitrary geometry
- Engineering novel complex scattering media

Delocalization in 1D Anderson Model

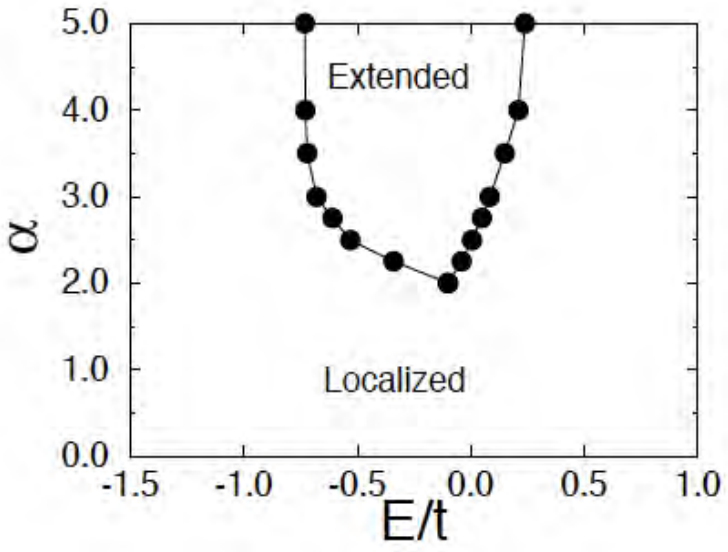

Long-Range Correlated potentials prevent Anderson Localization in 1D structures

De Moura and Lyra, PRL 81 17 (1998)

Structural Correlations in amorphous photonic media

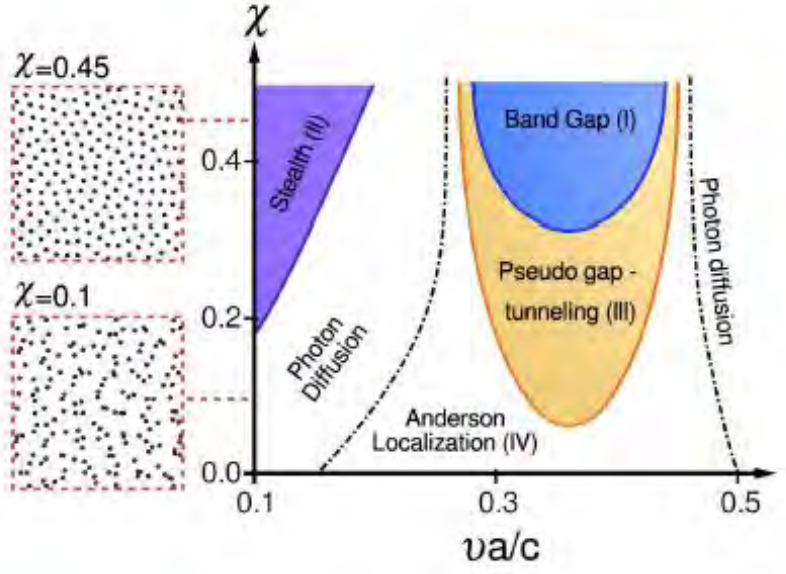

Correlation-frequency transport phase diagram for hyper-uniform disordered dielectric materials

Perez,et al, PNAS 114, 36 (2017)

Chain Length and Correlation Degree

Test of the structural correlation degree as a function of chain length (number of points) and number of realizations

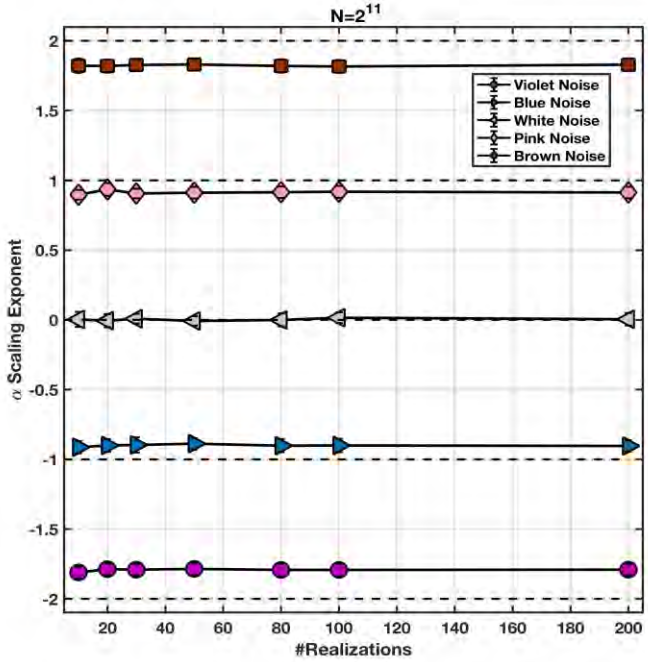

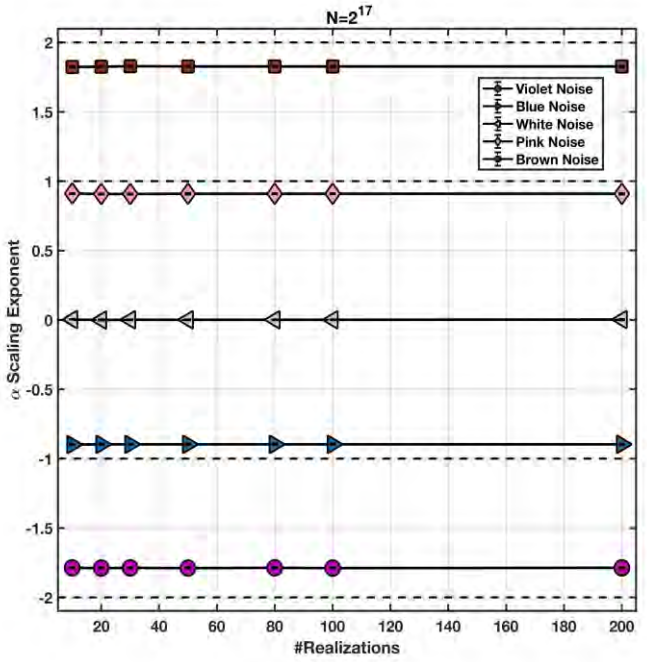

In our photonic implementation, the correlations were considered as perturbation with respect to a periodic configuration

$$x_n(\alpha) = d_0 n + \Xi\ \eta(\alpha)$$

Ξ is the modulation efficiency

$\eta(\alpha)$ Correlated sequence

F.Sgrignuoli, *et al*, in preparation (2018)

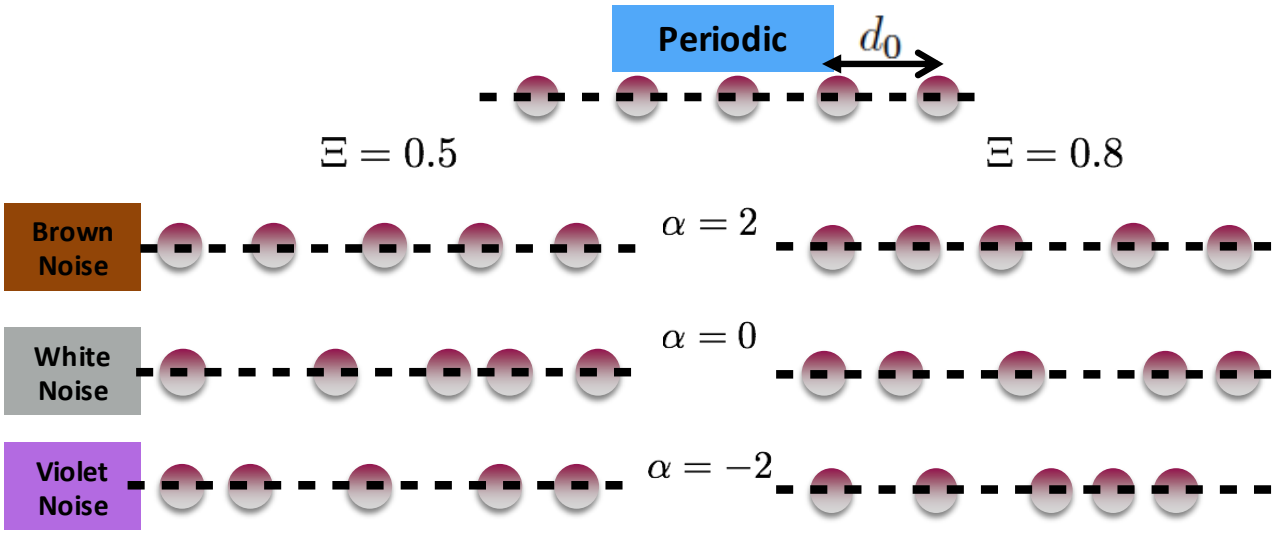

Eigenvalues Distribution (Ξ=0.5 and N=2^{11})

Brown Noise $\alpha = 2$

Pink Noise $\alpha = 1$

White Noise $\alpha = 0$

Blue Noise $\alpha = -1$

Violet Noise $\alpha = -2$

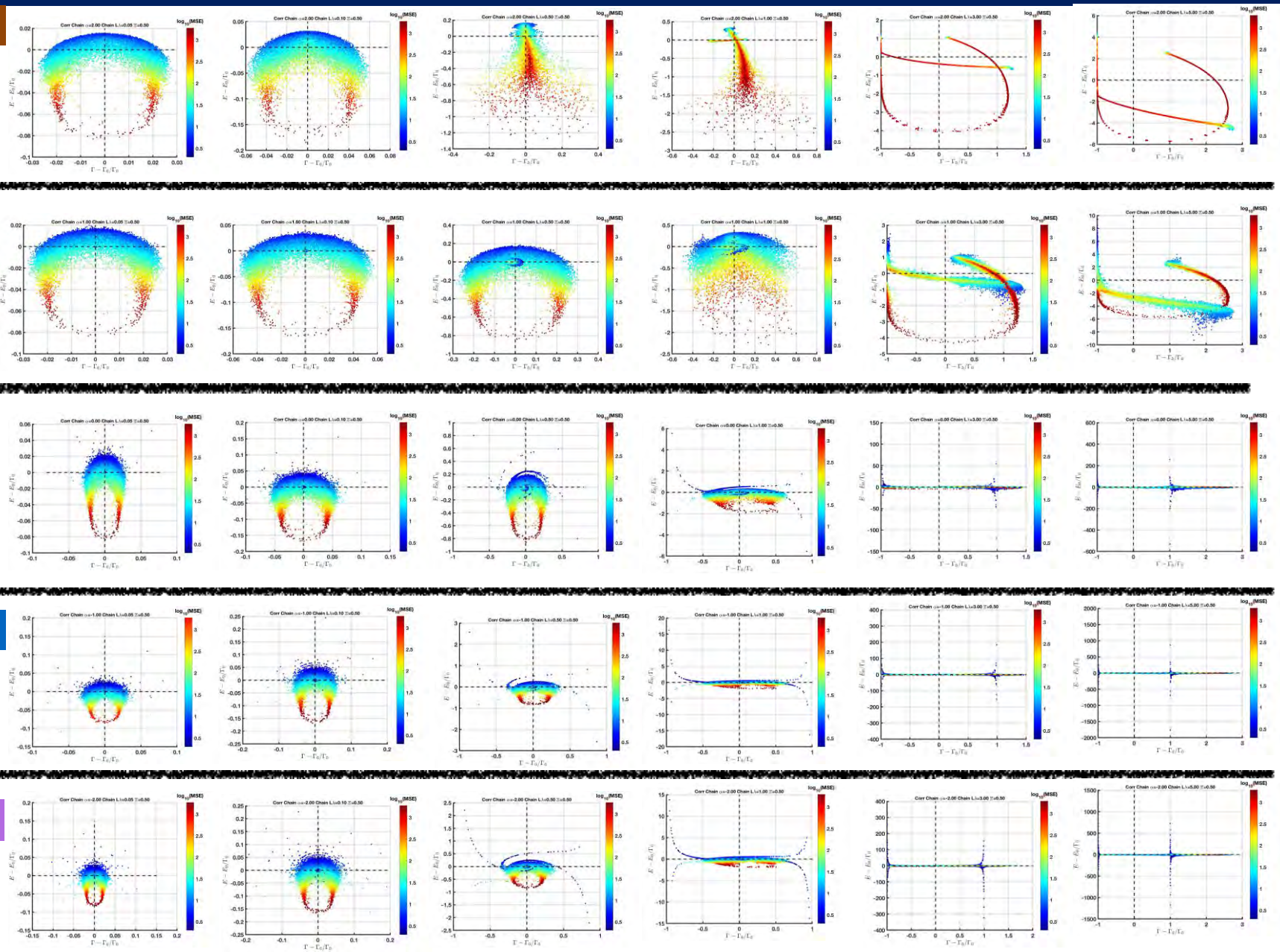

• OD=0.05 • OD=0.1 • OD=0.5 • OD=1 • OD=3 • OD=5

Level Spacing Statistics (Ξ=0.5 and N=2^{11}) bin=200

Brown Noise — $\alpha = 2$

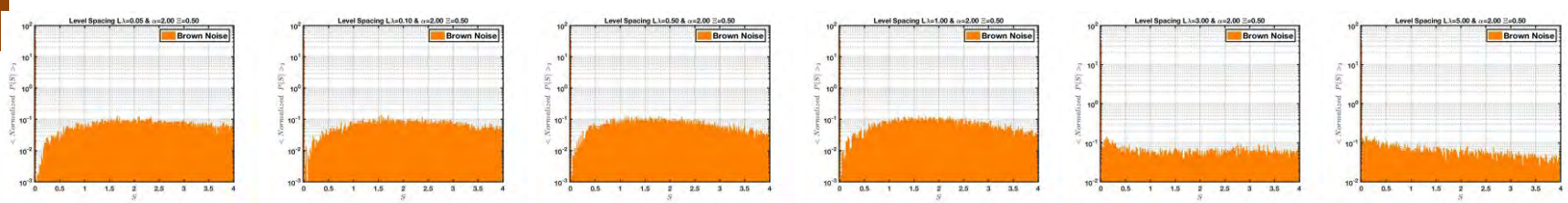

Pink Noise — $\alpha = 1$

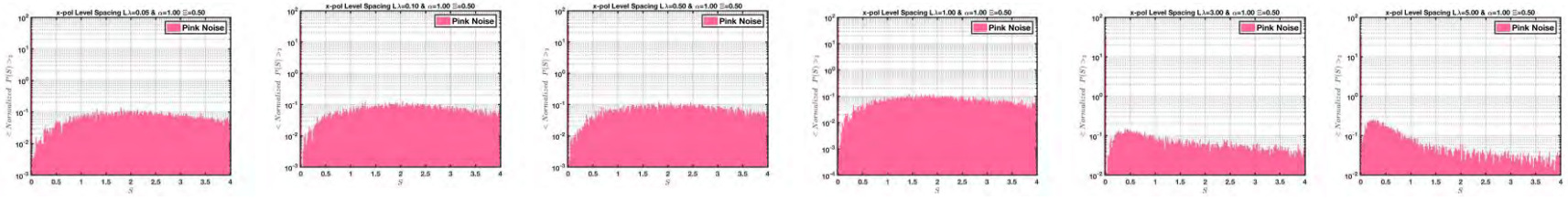

White Noise — $\alpha = 0$

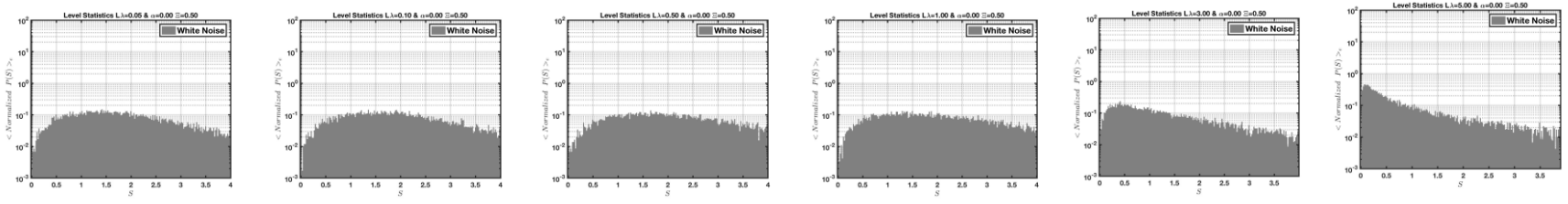

Blue Noise — $\alpha = -1$

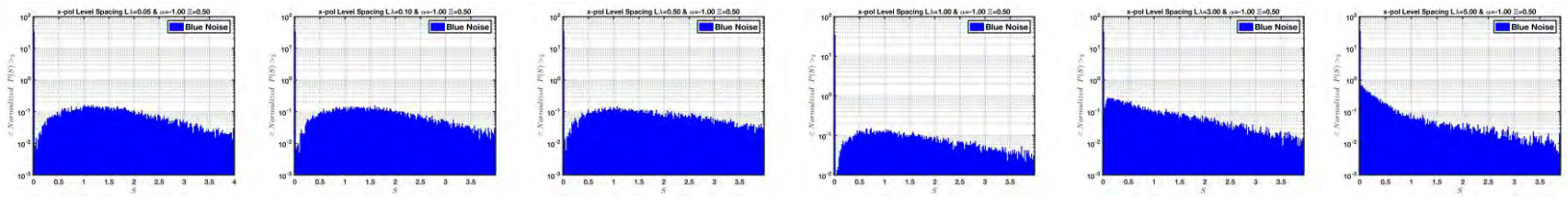

Violet Noise — $\alpha = -2$

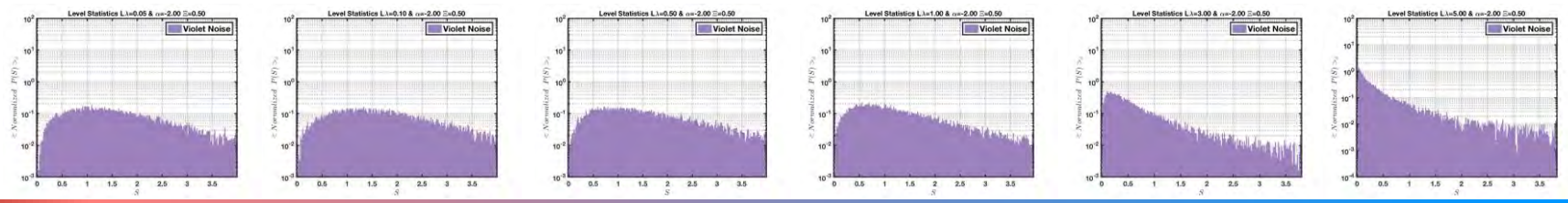

• OD=0.05 • OD=0.1 • OD=0.5 • OD=1 • OD=3 • OD=5

Future Plans

- Fabrication of Si-compatible doubly-negative metamaterials – BU and MITLL
  - Fabrication/characterization of core-shell structures
  - Planar fabrication of core-shell metamaterials and characterization
  - Demonstrate Si-compatible ENZ/MNZ materials in the 1-2μm range and $\chi^{(3)}$ nonlinearity enhancement
  - Experimental demonstration of k-space control in planar arrays of dielectric nanoparticles
- Nonlinear characterization @ BU
  - Second and Third Harmonic generation spectroscopy of nonlinear metamaterials
  - Z-scan (open/closed aperture) to measure nonlinear index modulation of ENZ and MNZ metamaterials
- See next slide for details for experimental capabilities in place at BU

Core-shell dielectric nanoparticles: fabrication routes

High index materials core
Silicon, Germanium

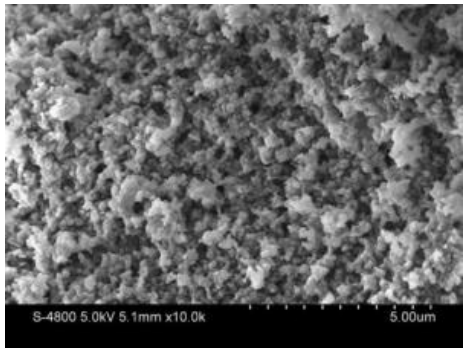

http://www.springpowerintl.com/?page_id=428

Conductive shell
ITO, Au, Ag

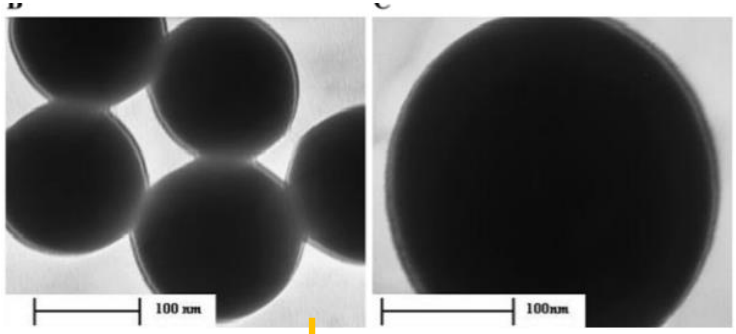

D. E. Michael, R. W. Eric, J Nanopart Res,14, 650;

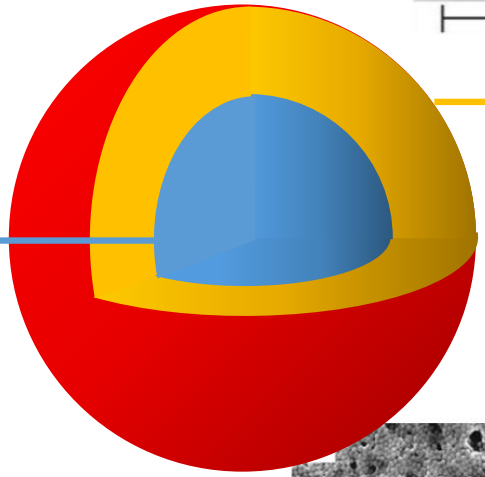

Layer by Layer deposition
of controlled thickness
Via reaction of precursor and
reducing reagent

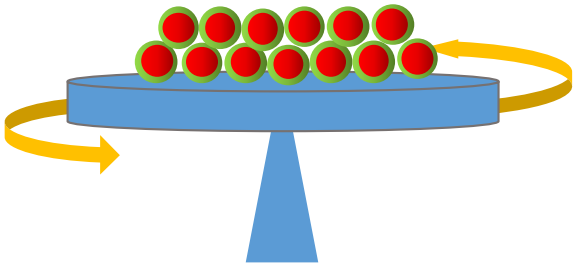

Multiple spin coating
or Dip coating
Forming uniform Core-shell
nanoparticles thick film

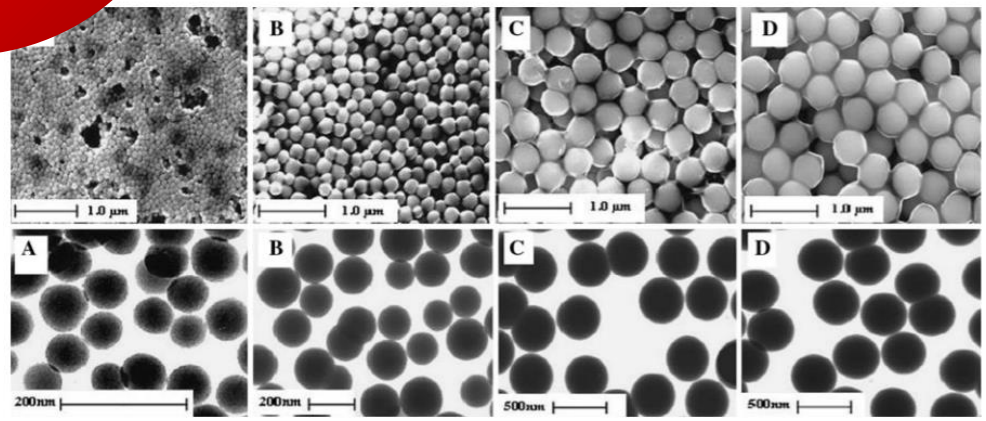

. S. G. Kim, N.Hagura, F. Iskandar, A. Yabuki, K. Okuyama. Thin Solid Films 516, 8721

Fabrication of core-shell nanoparticles at BU

Active Core component

Metal or semiconductor nanoparrticles

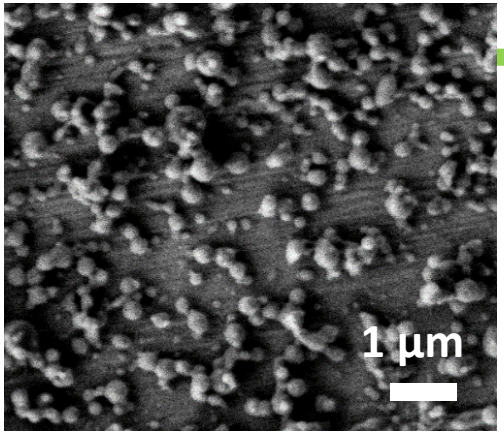

Core-shell nanoparticles

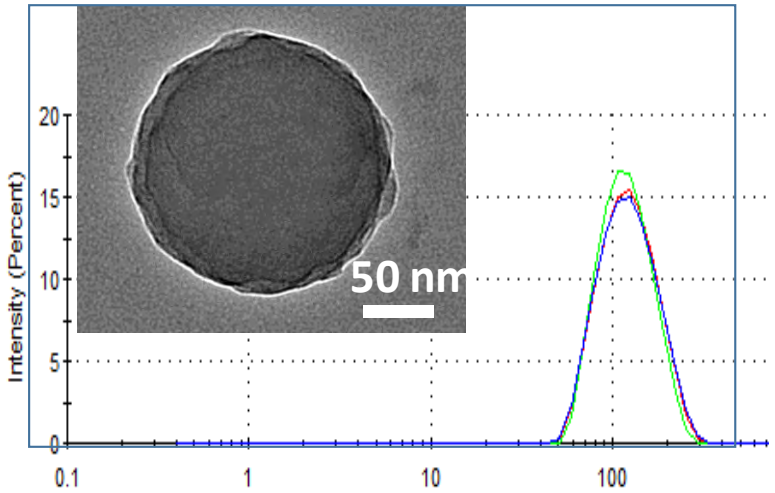

Shell component

PEG or ligand to for further deposition

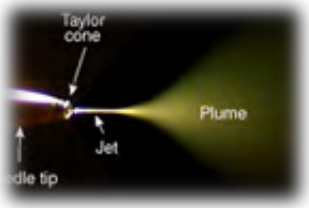

Electrospray

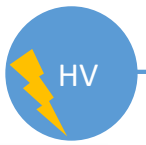

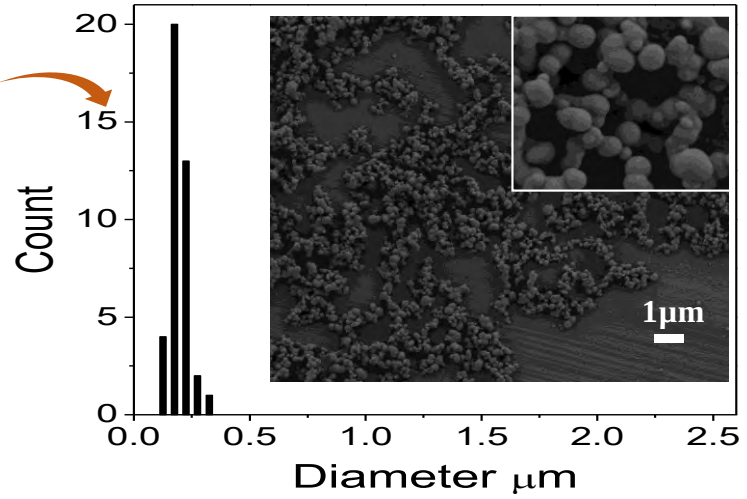

H. Sugimoto, R. Zhang, and L. Dal Negro, Appl. Phys. Lett., 107, 041111 (2015);

R. Zhang, S. Knitter, S. F. Liew, F. G. Omenetto, B.M. Reinhard, H. Cao and L. Dal Negro, Appl. Phys. Lett., 108, 011103 (2016).

R. Wang et al, in preparation (2018)

"To think without observing is as dangerous as observing without thinking" (S.R.y Cajal)

- **Nonlinear and ultrafast spectroscopy** (Mai Tai femtosecond laser, Spectra Physics OPO Inspire Auto 100, 100fs, 3W, wide tunability range 250nm-2500nm, GWU THG and FHG units for deep UV pulse generation), Hamamatsu picosecond streak camera, single photon counters, extended PMT tubes, Olympus IX7 Microscope / Andor Shamrock (750) Spectrometer).
- **Techniques available:** (Scattering/Absorption spectroscopy, time-resolved PL, SHG, THG, efficiency measurements, micro-Raman, photocurrent spectroscopy, pump-probe femtosecond, custom-made dark-field/bright-field microscope for the study of photonic/plasmonic nanostructures, dark-field microscopy).
- **Computational resources on our DURIP cluster** – 1000 AMD cores, Fast G-bit Interconnect
- **Materials deposition and nanofab:** magnetron sputtering, Ebeam litho., DRIE, electrospinning.